NATIONAL ADVISORY COMMITTEE FOR AERONAUTICS

TECHNICAL NOTE 2309

CHARTS FOR ESTIMATION OF LONGITUDINAL-STABILITY

DERIVATIVES FOR A HELICOPTER ROTOR

IN FORWARD FLIGHT

By Kenneth B. Amer and F. B. Gustafson

Langley Aeronautical Laboratory
Langley Field, Va.

NACA

Washington

March 1951

NATIONAL ADVISORY COMMITTEE FOR AERONAUTICS

———

TECHNICAL NOTE 2309

———

CHARTS FOR ESTIMATION OF LONGITUDINAL-STABILITY

DERIVATIVES FOR A HELICOPTER ROTOR

IN FORWARD FLIGHT

By Kenneth B. Amer and F. B. Gustafson

SUMMARY

    Charts are presented to provide a convenient means for obtaining
the derivatives of rotor resultant force, rotor pitching moment about
the helicopter center of gravity, and rotor torque with respect to rotor
angle of attack, forward speed, rotor speed, and collective pitch. The
analysis is made for untwisted, untapered blades which have flapping
hinges located at the rotor shaft. The charts can, however, be used
without serious error for blades with normal values of taper and twist
and means are indicated for obtaining the additional terms necessary when
the charts are applied to rotors having moderate flapping-hinge offsets.
These charts do not rely upon the assumption (often used for convenience)
that the rotor resultant-force vector is perpendicular to the tip-path
plane. This assumption is shown to lead often to grossly incorrect
longitudinal-stability derivatives.

    The method of using the charts to obtain the various derivatives is
explained and illustrated. The use of the charts in the study of the
general stability characteristics of the helicopter rotor is also
illustrated.

INTRODUCTION

    During the past few years, the factors that affect the performance
of the helicopter have become fairly well understood and, as a result,
the performance of the helicopter has been improved appreciably. Refer-
ences 1 and 2 indicate, however, that the flying qualities of helicopters
at the present time are still, in general, inferior to those of airplanes.
Reference 1 states that future Navy specifications will incorporate
stringent flying-qualities requirements for helicopters. According to
reference 2, the longitudinal flying qualities in forward flight are most
in need of improvement. Reference 3 presents tentative longitudinal

flying-qualities requirements based on the normal-acceleration charac-
teristics during a pull-up maneuver in forward flight. This reference
indicates that a helicopter that meets these requirements will be much
safer and less fatiguing to the pilot than one which does not.

In order to determine whether a prospective helicopter design will
meet the longitudinal flying-qualities requirements, stability calcu-
lations for a pull-up maneuver must be made. Such a calculation involves
setting up and solving simultaneously the differential equations of
motion of the helicopter. In order to set up these equations, the sta-
bility derivatives of the helicopter and, therefore, of the rotor must
be known. The stability derivatives are also useful for prediction of
other stability and control characteristics and for the study of stabi-
lizing devices and autopilots. In addition, these derivatives provide a
convenient basis for estimating load factors for arbitrary gust values.

The rotor theory of references 4 and 5 has been used for performance
and blade-motion calculations. These calculations have compared favor-
ably with flight test results (see, for example, references 6 and 7);
therefore, experimental checks are expected to show the same theory suit-
able for stability calculations. The results of reference 3 show that
this theory can be used for analytical studies of the ability of the
helicopter to meet the tentative longitudinal flying-qualities require-
ments of that reference. This theory, however, is presented in a form
convenient for performance and blade-motion studies but is not particularly
convenient for stability studies. Thus, a rework of the theory in order
to present it in a form more convenient for stability studies was con-
sidered desirable. For example, in estimating horizontal-tail area needed
to offset the angle-of-attack instability of a helicopter rotor, it was
found that, although the changes in magnitude of the rotor resultant-force
vector with angle of attack could readily be calculated, estimation of
the changes in vector longitudinal tilt with angle of attack to the
necessary degree of accuracy was relatively difficult. Approximation of
the vector longitudinal tilt by the easily calculated longitudinal flap-
ping a_1 appeared excessively inaccurate for the purpose. The basic
theory was accordingly used to prepare the charts presented herein from
which the values of the parameter a', which represents vector longitudinal
tilt, could be read directly. For convenience, values of torque coef-
ficient are also obtainable from these charts, and additional charts from
which variations in magnitude of the resultant-force vector can be read
directly are also included.

The charts presented herein can be conveniently used to obtain most
of the rotor longitudinal-stability derivatives. Those derivatives which
depend upon pitching velocity are not included in the present paper;
however, the damping moment due to a steady pitching velocity, which is
the most significant pitching-velocity derivative, can be obtained from
reference 8.

SYMBOLS

Physical Quantities

b   number of blades per rotor

r   radial distance to blade element, feet

R   blade radius, feet

c   blade-section chord, feet

c_e equivalent blade chord (on thrust basis), feet $\left(\dfrac{\displaystyle\int_0^R cr^2 dr}{\displaystyle\int_0^R r^2 dr} \right)$

σ rotor solidity $\left(bc_e/\pi R \right)$

θ blade-section pitch angle; angle between line of zero lift of blade section and plane perpendicular to axis of no feathering, radians

I_1 mass moment of inertia of blade about flapping hinge, slug-feet^2

ρ mass density of air, slugs per cubic foot

γ mass constant of rotor blade, expresses ratio of air forces to mass forces $\left(c\rho a R^4 / I_1 \right)$

δ_3 angle in plane of rotation between perpendicular to blade-span axis and flapping-hinge axis, positive when an increase in flapping produces a decrease in blade pitch

Air-Flow Parameters

V   true airspeed of helicopter along flight path, feet per second

V_h horizontal component of true airspeed of helicopter, feet per second

V_v vertical component of true airspeed of helicopter, feet
        per second

Ω rotor angular velocity, radians per second

α rotor angle of attack; angle between flight path and plane
        perpendicular to axis of no feathering, positive when axis
        is pointing rearward, radians

μ tip-speed ratio $\left(\dfrac{V \cos \alpha}{\Omega R} \text{ assumed equal to } \dfrac{V}{\Omega R}\right)$

v induced inflow velocity at rotor, always positive, feet
        per second

λ inflow ratio $\left(\dfrac{V \sin \alpha - v}{\Omega R}\right)$

ψ blade azimuth angle measured from downwind position in direc-
        tion of rotation, radians

U_T component at blade element of resultant velocity perpendicular
        to blade-span axis and to axis of no feathering, feet
        per second

$u_T = \dfrac{U_T}{\Omega R}$

U_P component at blade element of resultant velocity perpendicular
        both to blade-span axis and U_T, feet per second

ϕ inflow angle at blade element in plane perpendicular to blade-
        span axis, radians $\left(\tan^{-1} \dfrac{U_P}{U_T}\right)$

α_r blade-element angle of attack, measured from line of zero lift,
        radians $(\theta + \phi)$

<center>Aerodynamic Characteristics</center>

c_{d_o} section profile drag coefficient

a slope of curve of section lift coefficient against section
        angle of attack, per radian

L   rotor lift, pounds

T   rotor thrust, component of rotor resultant force parallel to
           axis of no feathering, pounds

Q   rotor-shaft torque, pound-feet

C_T rotor thrust coefficient $\left(\dfrac{T}{\pi R^2 \rho (\Omega R)^2}\right)$

C_Q rotor-shaft torque coefficient $\left(\dfrac{Q}{\pi R^2 \rho (\Omega R)^2 R}\right)$

Performance Parameters

$\left(\dfrac{D}{L}\right)_o$ rotor profile drag-lift ratio

$\left(\dfrac{D}{L}\right)_i$ rotor induced drag-lift ratio

$\left(\dfrac{D}{L}\right)_p$ parasite drag of helicopter components other than lifting
           rotors divided by rotor lift

$\left(\dfrac{D}{L}\right)_c$ drag-lift ratio representing angle of climb or glide, positive
           in climb $\left(V_v/V_h\right)$

$\left(\dfrac{D}{L}\right)_r$ rotor drag-lift ratio; ratio of equivalent drag of rotor to
           rotor lift $\left(\left(\dfrac{D}{L}\right)_o + \left(\dfrac{D}{L}\right)_i\right)$

$\left(\dfrac{D}{L}\right)_u$ component of rotor resultant force along flight path (that is,
           useful component of rotor resultant force) divided by rotor
           lift $\left(\left(\dfrac{D}{L}\right)_p + \left(\dfrac{D}{L}\right)_c\right)$

P/L shaft-power parameter, where P is equal to rotor-shaft power
           divided by velocity along flight path and is therefore also
           equal to drag force that could be overcome by shaft power
           at flight velocity $\left(\left(\dfrac{D}{L}\right)_r + \left(\dfrac{D}{L}\right)_u\right)$

ε angle of climb $\left(\tan^{-1} \dfrac{V_v}{V_h} = \tan^{-1} \left(\dfrac{D}{L}\right)_c\right)$

Rotor-Blade Motion

β blade flapping angle at particular azimuth position, radians

a_0 constant term in Fourier series that expresses β; therefore, rotor coning angle

a_1 coefficient of $-\cos\psi$ in expression for β; therefore, longitudinal tilt of rotor cone

b_1 coefficient of $-\sin\psi$ in expression for β; therefore, lateral tilt of rotor cone

Stability

a' projection of angle between rotor force vector and axis of no feathering in plane containing flight path and axis of no feathering

q helicopter pitching velocity, radians per second

Δ increment

$t_{a,b}$ functions of μ given in reference 4; subscripts a and b represent numbers used to identify a particular function

C parameter defined by equation (A10) in appendix A

STABILITY DERIVATIVES NEEDED FOR PULL-UP ANALYSIS

The stability derivatives needed for a pull-up analysis are now discussed, not only because of the significance of such an analysis but also because most of the derivatives needed for other longitudinal-stability studies are included in this relatively complex case. The actual use of these derivatives in a pull-up analysis is not discussed herein.

Rotor forces and blade flapping are affected by five independent variables: rotor angle of attack α, forward speed V, rotational speed Ω, collective pitch θ, and pitching velocity q. The helicopter is affected by both the magnitude and direction of the rotor resultant force and by the magnitude of the rotor torque. (The rotor resultant-force

vector is assumed to pass through the rotor hub inasmuch as present-day conventional rotors are designed with near-zero airfoil pitching moments and with coinciding aerodynamic centers and chordwise centers of gravity.) If the flapping hinges are offset from the rotor shaft or cocked, the helicopter will also be affected by longitudinal and lateral flapping and coning-angle changes. The magnitude and longitudinal direction of the rotor resultant force depend upon C_T/σ and a', respectively, and the magnitude of the rotor torque depends upon C_Q/σ. Calculation of the helicopter stability derivatives needed for a pull-up analysis therefore requires knowledge of the following rotor derivatives:

$$\frac{\partial(C_T/\sigma)}{\partial\alpha} \qquad \frac{\partial(C_T/\sigma)}{\partial V} \qquad \frac{\partial(C_T/\sigma)}{\partial\Omega} \qquad \frac{\partial(C_T/\sigma)}{\partial\theta} \qquad \frac{\partial(C_T/\sigma)}{\partial q}$$

$$\frac{\partial a'}{\partial\alpha} \qquad \frac{\partial a'}{\partial V} \qquad \frac{\partial a'}{\partial\Omega} \qquad \frac{\partial a'}{\partial\theta} \qquad \frac{\partial a'}{\partial q}$$

$$\frac{\partial(C_Q/\sigma)}{\partial\alpha} \qquad \frac{\partial(C_Q/\sigma)}{\partial V} \qquad \frac{\partial(C_Q/\sigma)}{\partial\Omega} \qquad \frac{\partial(C_Q/\sigma)}{\partial\theta} \qquad \frac{\partial(C_Q/\sigma)}{\partial q}$$

$$\frac{\partial a_1}{\partial\alpha} \qquad \frac{\partial a_1}{\partial V} \qquad \frac{\partial a_1}{\partial\Omega} \qquad \frac{\partial a_1}{\partial\theta} \qquad \frac{\partial a_1}{\partial q}$$

$$\frac{\partial a_0}{\partial\alpha} \qquad \frac{\partial a_0}{\partial V} \qquad \frac{\partial a_0}{\partial\Omega} \qquad \frac{\partial a_0}{\partial\theta} \qquad \frac{\partial a_0}{\partial q}$$

$$\frac{\partial b_1}{\partial\alpha} \qquad \frac{\partial b_1}{\partial V} \qquad \frac{\partial b_1}{\partial\Omega} \qquad \frac{\partial b_1}{\partial\theta} \qquad \frac{\partial b_1}{\partial q}$$

By definition, each partial derivative is obtained by assuming the other four independent variables to be constant.

All the preceding C_T/σ, a', and C_Q/σ derivatives, except those with respect to q, are obtainable from the charts in this paper. The a_0, a_1, and b_1 derivatives, except those with respect to q, can be obtained from the equations of reference 4. Although reference 4 is restricted to the case of flapping hinges on the rotor shaft, the equations are believed to be reasonably accurate for small values of flapping-hinge offset. The derivatives with respect to q are not included in the present paper; however, the changes in a' and a_1 due to a steady pitching velocity, which are the most significant pitching-velocity derivatives, can be obtained from reference 8.

For specific helicopter configurations, many of these derivatives may be expected to be insignificant, but no specific investigation of this possibility has yet been made.

For certain longitudinal-stability calculations, other rotor aerodynamic derivatives are desired. For example, in order to determine the rotor contribution to the variation of stick position with speed at fixed pitch, thrust, and rotational speed, the derivative $\partial a'/\partial V$ at constant C_T/σ (instead of at constant a) is needed. This a' derivative can also be obtained from the charts in this paper. Similarly, $\partial a'/\partial \Omega$ and $\partial a'/\partial \theta$, as well as the derivatives of C_Q/σ with respect to V, Ω, and θ, can be obtained at constant C_T/σ from the charts presented herein.

ASSUMPTIONS OF THEORY

In order to limit the labor involved in the theoretical derivations necessary to prepare the charts of this paper, various assumptions were made. For the readers' convenience, the more significant assumptions carried over from references 4 and 5 as well as those made herein are discussed.

Rotor Physical Characteristics

The rotor is assumed to have freely flapping rectangular untwisted blades with mass factor γ of 15 and the flapping hinge is assumed to be on the rotor shaft perpendicular to the blade-span axis. The charts, however, are considered applicable to rotors with blades having a range of γ from 0 to 25, moderate amounts of twist or taper, and moderate amounts of flapping-hinge offset or angularity $\left(\delta_3 \text{ angle}\right)$.

The consideration that the charts are applicable to rotors having values of γ ranging from 0 to 25 is based on the fact that the theory is shown in reference 4 to be applicable to this range of γ when a value of $\gamma = 15$ is used. The fact that the theory is satisfactory over this wide range of γ, and therefore for a variety of values of coning angle, lateral flapping angle, and of higher harmonics of flapping, suggested that it might be applicable to see-saw rotor systems. Further investigation of the problem indicated that the charts presented herein should, in general, give sufficiently accurate results for see-saw rotor systems.

The charts are considered applicable to rotors having moderate amounts of taper because the satisfactory comparison between calculated and measured rotor performance and blade motion previously referred to was obtained with blades which actually had a moderate amount of taper. The taper was accounted for theoretically by basing the solidity σ and the blade mass factor γ on an equivalent blade chord. (See "Symbols.")

The consideration that the charts are also applicable to rotors having moderate amounts of twist is based on a comparison made between the charts presented herein and calculations for a rotor with -8° of linear twist. This comparison showed that the C_T/σ derivatives are not significantly affected. The absolute values of a' given by the charts are nowhere in error by more than 1° and rotor instability with angle of attack is indicated to be somewhat high, which is conservative. The other a' derivatives and the C_Q/σ derivatives for the rotor with -8° twist are given by the charts to a satisfactory degree of engineering accuracy.

The applicability of the charts to rotors with moderate amounts of flapping-hinge offset is logically justified as follows. Small amounts of flapping-hinge offset (less than 5 percent R) are not considered likely to affect rotor performance. Thus, inasmuch as the charts presented herein are derived from performance equations, they should be applicable without excessive error to rotors having flapping-hinge offsets of less than 5 percent of the rotor radius. For such rotors, however, the effect of longitudinal flapping with respect to the shaft in producing additional pitching moments due to the centrifugal force in the blades must be taken into account.

The charts can be applied to rotors having angular flapping hinges (δ_3 angle) if the resulting effect of lateral flapping on the longitudinal position of the axis of no feathering is taken into account. (The axis of no feathering is the axis about which no first harmonic pitch variation occurs. See appendix of reference 7 for discussion of its use and significance.)

Section Aerodynamic Characteristics

The equation representing the blade-section profile drag coefficient is

$$c_{d_0} = 0.0087 - 0.0216\alpha_r + 0.400\alpha_r^2$$

Comparisons between this theoretical profile drag polar and statically measured experimental polars for several typical airfoils are given in figure 1 of reference 5. This theoretical polar can also be compared with

statically measured drag polar data presented in reference 9. The sec-
tion is assumed to have a lift-curve slope of 5.73 per radian. This
value can be compared with statically measured lift curves of various
rotor-blade airfoil sections which are also presented in reference 9.

These lift and drag section characteristics are assumed to be con-
stant over the rotor disk; that is, effects of radial velocities and
variations around the disk in Reynolds number and Mach number are
neglected.

Rotor Aerodynamic Characteristics

In the calculation of rotor aerodynamic characteristics from the
blade-section characteristics, the inflow velocity is assumed to be

uniform and θ, $\emptyset$, a_r, β, α, $\tan^{-1}\left(\dfrac{D}{L}\right)_u$, and a' are assumed to be
small angles so that the sine is equal to the angle and the cosine is
unity. The charts are limited to values of μ between 0.15 and 0.50
where these assumptions are believed to be valid. The most questionable
assumption is that of uniform inflow velocity. This assumption is con-
sidered reasonable for calculating longitudinal-stability derivatives in
view of the previously referred to satisfactory comparisons between rotor
theory based on this assumption and both measured longitudinal flapping
and rotor performance.

The loss in lift at the tip of the blade is approximated in cal-
culating rotor aerodynamic characteristics by assuming that the outer
3 percent of the blade radius is ineffective in producing lift but does
produce drag.

In calculations of rotor thrust, the contribution of blade-section
drag is omitted as being negligible.

LIMITS OF VALIDITY OF THEORY

Stalling Limits

As was explained in references 4 and 5, the accuracy of the theory
becomes doubtful when a stalling angle of attack is encountered at $\psi = 270°$
by either a section at the blade tip or by an inboard section with relative
velocity equal to four-tenths the rotational tip speed. The reasons for
this doubtful accuracy are that the theory fails to take account of the
nonlinearity of the lift curve and the increased drag rise at the stall.

The charts of this paper, therefore, follow the procedure of the charts of reference 5 in that locus lines for 12° and 16° angles of attack are included. The locus lines for the conditions for which a blade element at an azimuth angle of 270° with a relative velocity $u_T\Omega R$ equal to four-tenths the rotational tip speed reaches a specified angle of attack are designated by the symbol $\alpha_{(u_T=0.4)(270°)}$. Similarly, the locus lines for the conditions for which the blade tip at an azimuth angle of 270° reaches a specified angle of attack are designated by the symbol $\alpha_{(1.0)(270°)}$. Inasmuch as a rotor with twisted blades has approximately the same pitch at the three-quarter radius as a rotor with untwisted blades for the same flight condition, the specified angles on the tip locus lines should be reduced by approximately one-fourth of the blade twist value when using the charts for twisted blades. A similar correction that depends upon μ can be calculated for the specified angles on the locus lines for $u_T = 0.4$.

As pointed out in several previous NACA papers (see, for example, reference 5), the optimum flight condition from considerations of helicopter performance is approximately that at which stalling just begins. A helicopter designed to fly near this optimum performance condition therefore always enters the stalled region during an appreciable pull-up or upward gust. It would therefore be desirable to determine the necessary empirical correction, if any, to the stalled part of the charts presented herein. This correction, however, is believed to be beyond the scope of the present paper.

Mach Number Limits

Although the section lift and drag characteristics vary with Mach number, on the basis of performance prediction experience, it is believed that such changes would not significantly affect the validity of the charts presented herein (except perhaps fig. 1(a)) at least until the Mach number for lift and drag divergence is reached. It is possible that these charts may be valid somewhat beyond this point because of a tip-relief effect and other factors, but further discussion of this point is believed to be beyond the scope of this paper.

The quantities given in figure 1(a) are more directly dependent on lift-curve slope and, for helicopters with unusually high tip speeds, the effect of Mach number may be significant even before the lift divergence is reached. For such designs, the average section lift-curve slope may be appreciably higher than the value of 5.73 used herein. If such is the case, equations given in appendix A may be used in place of figure 1(a) for greater accuracy.

Rotor Angle-of-Attack Limits

Inasmuch as the term $\cos\alpha$ occurs in the accurate expression for μ, a change in rotor angle of attack while constant forward speed

and rotor speed are maintained causes a small change in μ. This change in μ in turn causes a small correction to the derivatives with respect to α as calculated with $\cos \alpha$ assumed to equal 1.0. If desired, this correction is obtained as follows:

$$\mu = \frac{V \cos \alpha}{\Omega R}$$

Differentiating this expression yields

$$\left(\frac{\partial \mu}{\partial \alpha}\right)_{\text{const. } V, \Omega} = -\frac{V \sin \alpha}{\Omega R} = -\mu \tan \alpha$$

Therefore,

$$\left(\frac{\partial}{\partial \alpha}\right)_{\text{const. } V} = \left(\frac{\partial}{\partial \alpha}\right)_{\text{const. } \mu} - \mu \tan \alpha \frac{\partial}{\partial \mu} \tag{1}$$

Calculations indicate that the rotor angle of attack is usually small enough to make this correction term insignificant.

Need for Experimental Verification

Because of the various assumptions used in the theory on which the charts presented herein are based, adequate experimental verification is necessary before these charts can be used with complete confidence. Only approximate and incomplete experimental checks are as yet available. Nevertheless, because of the satisfactory correlation of experiment and theory for rotor performance and blade motion previously referred to and because of the satisfactory comparison between measured and predicted pull-up time histories shown in reference 3, it is believed that these charts can be used with some confidence even before any further experimental verification is obtained.

DERIVATION OF CHARTS

C_T/σ Derivatives

The C_T/σ derivatives are obtained by combining equations (6) and (7) of reference 4, which (with the blade-twist term dropped) are, respectively,

$$\frac{2C_T}{\sigma a} = t_{3,1}\lambda + t_{3,2}\theta$$

and

$$\tan \alpha = \frac{\lambda}{\mu} + \frac{C_T}{2\mu\left(\lambda^2 + \mu^2\right)^{1/2}}$$

(The symbols such as $t_{3,1}$ refer to tabulated constants in reference 4. The subscript designates the table number and line. For a rotor with twisted blades, θ is approximately the pitch at the three-quarter radius.)

The manner in which these equations are combined and processed is described in appendix A. As explained in that appendix, typical values of λ and C_T are employed in obtaining figures 1(a) and 1(b) ($\lambda = -0.05$, $C_T = 0.005$). Calculations indicate that, for $\mu \geqq 0.15$, this approximation should seldom involve any significant error but, for special cases, the equations given in appendix A can be employed.

Derivatives of C_T/σ with respect to θ and α.- The derivative $\dfrac{\partial\left(C_T/\sigma\right)}{\partial\theta}$ for constant μ and α and the derivative $\dfrac{\partial\left(C_T/\sigma\right)}{\partial\alpha}$ for constant μ and θ are plotted against μ in figure 1(a) for values of μ from 0.15 to 0.50 and for $\sigma = 0.03$, 0.06, and 0.09.

Derivative of $\left(C_T/\sigma\right)$ with respect to μ.- The derivative $\dfrac{\partial\left(C_T/\sigma\right)}{\partial\mu}$ for constant α and θ is given by the following equation:

$$\frac{\partial\left(C_T/\sigma\right)}{\partial\mu} = k_1\theta + k_2\frac{C_T}{\sigma} + k_3 C_T\theta^2 + k_4\frac{C_T^2\theta}{\sigma} + k_5\frac{C_T^3}{\sigma^2} \qquad (2)$$

where the k quantities are plotted against μ in figure 1(b) for values of μ from 0.15 to 0.50 and for $\sigma = 0.03$, 0.06, and 0.09.

a' and C_Q/σ Derivatives

Figure 2 shows that the longitudinal angle between the rotor resultant-force vector and the axis of no feathering is

$$a' = -\left[\arc\tan\left(\frac{D}{L}\right)_u + \alpha\right] \qquad (3)$$

Therefore, use of the trigonometric formula for the tangent of a sum of two angles gives

$$\tan a' = -\frac{\left(\frac{D}{L}\right)_u + \tan \alpha}{1 - \left(\frac{D}{L}\right)_u \tan \alpha} \tag{4}$$

Substituting equation (7) of reference 4 and equation (1) of reference 5 gives

$$\tan a' = \frac{\left(\frac{D}{L}\right)_o + \left(\frac{D}{L}\right)_i - \frac{P}{L} - \frac{\lambda}{\mu} - \frac{C_T}{2\mu\sqrt{\mu^2 + \lambda^2}}}{1 - \left(\frac{D}{L}\right)_u \tan \alpha} \tag{5}$$

According to the second term of equation (11-4) of reference 10,

$$\left(\frac{D}{L}\right)_i = \frac{C_T}{2\mu\sqrt{\mu^2 + \lambda^2}}$$

Thus,

$$\tan a' = \frac{\left(\frac{D}{L}\right)_o - \frac{P}{L} - \frac{\lambda}{\mu}}{1 - \left(\frac{D}{L}\right)_u \tan \alpha} \tag{6}$$

Substituting for λ from equation (6) of reference 4 (dropping the blade-twist term) results in the following equation:

$$\tan a' = \frac{\left(\frac{D}{L}\right)_o - \frac{P}{L} + \frac{t_{3,2}\theta - \frac{2C_T}{\sigma a}}{\mu t_{3,1}}}{1 - \left(\frac{D}{L}\right)_u \tan \alpha} \tag{7}$$

Assuming that a', α, and $\arc\tan\left(\dfrac{D}{L}\right)_u$ are small angles, a' can be expressed in degrees as follows:

$$a'^\circ = 57.3\left[\left(\frac{D}{L}\right)_o - \frac{P}{L}\right] + \frac{t_{3,2}\theta^\circ - 57.3\,\dfrac{2C_T}{\sigma a}}{t_{3,1}\mu} \tag{8}$$

The angle a'° can be calculated from equation (8) as a function of μ, C_T/σ, and θ by first calculating $(D/L)_o$ and P/L as functions of μ, C_T/σ, and θ from the equations of reference 4 as was done to obtain the charts of reference 5. The results of these calculations for a' are plotted in figure 3, which also includes lines of constant P/L. Thus, figure 3 can be used to obtain a' and C_Q/σ derivatives (C_Q/σ being directly related to P/L). Each chart of figure 3 is for a constant value of collective pitch, because this parameter is the one most likely to remain constant during a change in flight condition caused by a gust or maneuver.

The values of a' and P/L, rather than their derivatives, are plotted in figure 3 in order to keep the number of charts down to a minimum. Thus, slopes or differences must be measured and some simple calculation often must be made in order to obtain the a' and C_Q/σ derivatives from the charts of figure 3.

COMPARISON BETWEEN a' AND a_1

Because of the unavailability of a convenient source of a', most stability calculations have heretofore been made on the assumption that $a' = a_1$ because a_1 was much more readily calculated. The error caused by this assumption is shown in figure 4, which compares theoretical values of a' and a_1 for $\mu = 0.15$, 0.30, and 0.50 and $\theta = 0^\circ$, 8°, and 14°. In general, the comparison between the slopes or increments is quite unsatisfactory, and thus it is concluded that the substitution of a_1 for a' frequently yields grossly incorrect rotor stability derivatives.

METHOD OF OBTAINING STABILITY DERIVATIVES

The procedure for obtaining the rates of change of C_T/σ, a', and C_Q/σ with respect to α, V, Ω, and θ for a helicopter rotor in forward flight from the charts presented herein is as follows:

(1) The values of σ and R and the trim values of V, μ, C_T/σ, and P/L must be known. For cases where P/L is not already known, it can be obtained from the charts of reference 5.

(2) The value of collective pitch θ can be obtained either from the charts of reference 5 or by interpolating between the various charts of figure 3 presented herein. For a rotor with twisted blades, the collective pitch on the charts represents approximately the pitch at the three-quarter radius.

(3) The rates of change of thrust-coefficient – solidity ratio with rotor angle of attack and collective pitch angle are obtained from figure 1(a) where these two derivatives are plotted against tip-speed ratio for specified values of rotor solidity. (The upper curves of fig. 1(a) are accurate to within 4 percent and the lower curves are accurate to within 7 percent for λ from 0.05 to −0.10, C_T from 0.002 to 0.008, and α less than $10°$ in magnitude. For greater accuracy, equations (A5), (A10), and (A11) of appendix A can be used.)

(4) The rate of change of thrust-coefficient – solidity ratio with tip-speed ratio can be calculated by use of equation (2). The values of the five constants in equation (2) can be obtained from figure 1(b) where they are plotted against tip-speed ratio for specified values of solidity. (The curves of fig. 1(b) are accurate to within 4 percent for λ between 0.05 and −0.10 and C_T between 0.002 and 0.008. Also equation (2) assumes λ/μ to be less than 0.5 in magnitude. For greater accuracy, equations (A10) and (A15) of appendix A can be used.)

Derivatives with respect to V and Ω are then obtained as follows:

$$\frac{\partial\left(C_T/\sigma\right)}{\partial V} = \frac{\partial\mu}{\partial V}\,\frac{\partial\left(C_T/\sigma\right)}{\partial\mu} = \frac{1}{\Omega R}\,\frac{\partial\left(C_T/\sigma\right)}{\partial\mu} \tag{9}$$

and

$$\frac{\partial\left(C_T/\sigma\right)}{\partial\Omega} = \frac{\partial\mu}{\partial\Omega}\,\frac{\partial\left(C_T/\sigma\right)}{\partial\mu} = -\frac{\mu}{\Omega}\,\frac{\partial\left(C_T/\sigma\right)}{\partial\mu} \tag{10}$$

(5) Once the C_T/σ derivatives are known, the rates of change of longitudinal rotor-vector tilt and torque-coefficient – solidity ratio with respect to rotor angle of attack, tip-speed ratio (and, therefore, forward or rotational speed), and pitch setting can be obtained for various trim combinations of tip-speed ratio, thrust-coefficient – solidity ratio, and power input from figure 3, which consists of a series of charts for different values of pitch setting. In these charts, the longitudinal angle a' between the rotor resultant-force vector and the axis of no feathering is plotted against the thrust-coefficient – solidity ratio for specified values of tip-speed ratio. Lines of constant-power drag-lift ratio P/L, which is directly related to torque coefficient, are cross-plotted in the charts.

(6) The a' and C_Q/σ derivatives are obtained from figure 3 by measuring slopes or differences and using these quantities in the following formulas (sample derivations of these formulas are given in appendix B, and a sample problem is worked out in the section following this one):

$$\frac{\partial a'}{\partial \alpha} = \frac{\partial a'}{\partial (C_T/\sigma)} \frac{\partial (C_T/\sigma)}{\partial \alpha} \tag{11}$$

$$\left(\frac{\partial a'}{\partial V}\right)_{\text{const. } C_T/\sigma} = \frac{1}{\Omega R}\left(\frac{\partial a'}{\partial \mu}\right)_{\text{const. } C_T/\sigma} \tag{12}$$

$$\left(\frac{\partial a'}{\partial V}\right)_{\text{const. } \alpha} = \frac{1}{\Omega R}\left[\left(\frac{\partial a'}{\partial \mu}\right)_{\text{const. } C_T/\sigma} + \frac{\partial a'}{\partial (C_T/\sigma)} \frac{\partial (C_T/\sigma)}{\partial \mu}\right] \tag{13}$$

$$\left(\frac{\partial a'}{\partial \Omega}\right)_{\text{const. } C_T/\sigma} = -\frac{\mu}{\Omega}\left(\frac{\partial a'}{\partial \mu}\right)_{\text{const. } C_T/\sigma} \tag{14}$$

$$\left(\frac{\partial a'}{\partial \Omega}\right)_{\text{const. } \alpha} = -\frac{\mu}{\Omega}\left[\left(\frac{\partial a'}{\partial \mu}\right)_{\text{const. } C_T/\sigma} + \frac{\partial a'}{\partial (C_T/\sigma)} \frac{\partial (C_T/\sigma)}{\partial \mu}\right] \tag{15}$$

$$\left(\frac{\partial a'}{\partial \theta}\right)_{\text{const. } C_T/\sigma} = \frac{\Delta a'}{\Delta \theta} \tag{16}$$

(The values of $\Delta a'$ and $\Delta \theta$ are obtained from two adjacent charts for θ at an appropriate combination of μ and C_T/σ.)

$$\left(\frac{\partial a'}{\partial \theta}\right)_{\text{const. } \alpha} = \left(\frac{\partial a'}{\partial \theta}\right)_{\text{const. } C_T/\sigma} + \frac{\partial a'}{\partial (C_T/\sigma)} \frac{\partial (C_T/\sigma)}{\partial \theta} \qquad (17)$$

$$\frac{\partial (C_Q/\sigma)}{\partial \alpha} = \mu \frac{\partial (C_T/\sigma)}{\partial \alpha}\left[\frac{P}{L} + \frac{C_T}{\sigma} \frac{\partial (P/L)}{\partial (C_T/\sigma)}\right] \qquad (18)$$

$$\left[\frac{\partial (C_Q/\sigma)}{\partial \theta}\right]_{\text{const. } C_T/\sigma} = \mu \frac{C_T}{\sigma}\left[\frac{\partial (P/L)}{\partial \theta}\right]_{\text{const. } C_T/\sigma} \qquad (19)$$

$$\left[\frac{\partial (C_Q/\sigma)}{\partial \theta}\right]_{\text{const. } \alpha} = \mu \frac{\partial (C_T/\sigma)}{\partial \theta}\left[\frac{P}{L} + \frac{C_T}{\sigma} \frac{\partial (P/L)}{\partial (C_T/\sigma)}\right] + \mu \frac{C_T}{\sigma}\left[\frac{\partial (P/L)}{\partial \theta}\right]_{\text{const. } C_T/\sigma} \qquad (20)$$

$$\left[\frac{\partial (C_Q/\sigma)}{\partial V}\right]_{\text{const. } C_T/\sigma} = \frac{C_T/\sigma}{\Omega R}\left\{\frac{P}{L} + \mu\left[\frac{\partial (P/L)}{\partial \mu}\right]_{\text{const. } C_T/\sigma}\right\} \qquad (21)$$

$$\left[\frac{\partial (C_Q/\sigma)}{\partial \Omega}\right]_{\text{const. } C_T/\sigma} = -\frac{\mu C_T/\sigma}{\Omega}\left\{\frac{P}{L} + \mu\left[\frac{\partial (P/L)}{\partial \mu}\right]_{\text{const. } C_T/\sigma}\right\} \qquad (22)$$

$$\left[\frac{\partial (C_Q/\sigma)}{\partial V}\right]_{\text{const. } \alpha} = \frac{C_T/\sigma}{\Omega R}\left\{\frac{P}{L} + \mu\left[\frac{\partial (P/L)}{\partial \mu}\right]_{\text{const. } C_T/\sigma}\right\} + \qquad (23)$$

$$\frac{\mu}{\Omega R} \frac{\partial (C_T/\sigma)}{\partial \mu}\left[\frac{P}{L} + \frac{C_T}{\sigma} \frac{\partial (P/L)}{\partial (C_T/\sigma)}\right]$$

$$\left[\frac{\partial(C_Q/\sigma)}{\partial\Omega}\right]_{\text{const. }\alpha} = -\frac{\mu C_T/\sigma}{\Omega}\left\{\frac{P}{L} + \mu\left[\frac{\partial(P/L)}{\partial\mu}\right]_{\text{const. }C_T/\sigma}\right\} -$$

$$\frac{\mu^2}{\Omega}\frac{\partial(C_T/\sigma)}{\partial\mu}\left[\frac{P}{L} + \frac{C_T}{\sigma}\frac{\partial(P/L)}{\partial(C_T/\sigma)}\right]$$

(24)

SAMPLE ROTOR LONGITUDINAL-STABILITY-DERIVATIVE CALCULATIONS

In this section, the longitudinal-stability derivatives, which experience has thus far indicated to be significant (except those with respect to pitching velocity), are calculated for the rotor for the sample helicopter of reference 5 by use of the methods indicated in the previous section. The procedure for calculating any of the other stability derivatives discussed in the previous section are then readily deducible and thus are not specifically discussed. For the sample helicopter,

σ 0.07

R, feet 20

V, feet per second 80

μ 0.20

P/L 0.20

C_T/σ 0.094

Determination of P/L and θ

For cases where P/L is not already available from performance calculations or measurements, it can be readily obtained by the method illustrated in reference 5. If the charts of reference 5 are used for this purpose, the collective pitch θ which is needed for some of the derivatives can conveniently be determined at the same time. Because P/L is already known for this sample problem, θ can be obtained from figure 3. Interpolation between the charts for $\theta = 8°$ and $\theta = 10°$ and use of the known values of μ, C_T/σ, and P/L gives

$$\theta = 9.2° = 0.160 \text{ radian}$$

If the sample rotor has twisted blades, this pitch value is the value of pitch at approximately the three-quarter radius.

$$C_T/\sigma \quad \text{Derivatives}$$

From figure 1(a),

$$\frac{\partial\left(C_T/\sigma\right)}{\partial\alpha} = 0.23 \text{ per radian}$$

$$\frac{\partial\left(C_T/\sigma\right)}{\partial\theta} = 0.76 \text{ per radian}$$

From equation (2) and figure 1(b),

$$\frac{\partial\left(C_T/\sigma\right)}{\partial\mu} = -3.4(0.160) + 6.2(0.094) - 3.1(100)(0.094)(0.07)(0.16)^2 +$$

$$0.7(1000)(0.094)^2(0.07)(0.160) - 3.6(100)(0.094)^3(0.07)$$

$$\frac{\partial\left(C_T/\sigma\right)}{\partial\mu} = 0.04$$

$$\Omega R = \frac{V}{\mu} = 400 \text{ feet per second}$$

$$\Omega = \frac{400}{20} = 20 \text{ radians per second}$$

From equations (9) and (10),

$$\frac{\partial\left(C_T/\sigma\right)}{\partial V} = \frac{0.04}{400} = 0.0001 \text{ per foot per second}$$

$$\frac{\partial\left(C_T/\sigma\right)}{\partial\Omega} = \left(-\frac{0.2}{20}\right)(0.04) = -0.0004 \text{ per radian per second}$$

$$a' \quad \text{and} \quad C_Q/\sigma \quad \text{Derivatives}$$

$\frac{\partial a'}{\partial\alpha}$ derivative.- Interpolation between the charts for $\theta = 8°$ and $\theta = 10°$ of the slopes of the lines for $\mu = 0.20$ gives

$$\frac{\partial a'}{\partial\left(C_T/\sigma\right)} = 29° = 0.51 \text{ radian}$$

Using equation (11) yields

$$\frac{\partial a'}{\partial \alpha} = (0.51)(0.23) = 0.12 \text{ radian per radian}$$

$\frac{\partial a'}{\partial V}$ derivative at constant C_T/σ.- Interpolation between the charts for $\theta = 8°$ and $\theta = 10°$ of the increment in a' from $\mu = 0.15$ to $\mu = 0.25$ at $\frac{C_T}{\sigma} = 0.094$ gives

$$\left(\frac{\partial a'}{\partial \mu}\right)_{\text{const. } C_T/\sigma} = 22° = 0.38 \text{ radian}$$

Using equation (12) yields

$$\left(\frac{\partial a'}{\partial V}\right)_{\text{const. } C_T/\sigma} = \frac{0.38}{400} = 0.00095 \text{ radian per foot per second}$$

$\frac{\partial a'}{\partial V}$ derivative at constant α.- Using equation (13) yields

$$\left(\frac{\partial a'}{\partial V}\right)_{\text{const. } \alpha} = \frac{1}{400}\Big[0.38 + (0.51)(0.04)\Big] = 0.0010 \text{ radian per foot per second}$$

$\frac{\partial\left(C_Q/\sigma\right)}{\partial \alpha}$ derivative.- Interpolation between the charts for $\theta = 8°$ and $\theta = 10°$ of the increment in P/L from $\frac{C_T}{\sigma} = 0.084$ to $\frac{C_T}{\sigma} = 0.104$ along the lines for $\mu = 0.20$ gives

$$\frac{\partial(P/L)}{\partial\left(C_T/\sigma\right)} = -4.8$$

Using equation (18) yields

$$\frac{\partial\left(C_Q/\sigma\right)}{\partial \alpha} = (0.20)(0.23)\Big[0.20 + (0.094)(-4.8)\Big] = -0.012 \text{ per radian}$$

$\dfrac{\partial\left(C_Q/\sigma\right)}{\partial\theta}$ derivative at constant C_T/σ.- Comparison between the charts

for $\theta = 8°$ and $\theta = 10°$ at $\mu = 0.20$ and $\dfrac{C_T}{\sigma} = 0.094$ gives

$$\left[\frac{\partial(P/L)}{\partial\theta}\right]_{\text{const. } C_T/\sigma} = \frac{0.253 - 0.137}{\dfrac{2}{57.3}} = 3.3 \text{ per radian}$$

Using equation (19) yields

$$\left[\frac{\partial\left(C_Q/\sigma\right)}{\partial\theta}\right]_{\text{const. } C_T/\sigma} = 0.20(0.094)(3.3) = 0.062 \text{ per radian}$$

$\dfrac{\partial\left(C_Q/\sigma\right)}{\partial\theta}$ derivative at constant α.- Using equation (20) yields

$$\left[\frac{\partial\left(C_Q/\sigma\right)}{\partial\theta}\right]_{\text{const. } \alpha} = 0.20(0.76)\Big[0.20 + 0.094(-4.8)\Big] + 0.20(0.094)(3.3)$$

$$= -0.038 + 0.062$$

$$= 0.024 \text{ per radian}$$

$\left[\dfrac{\partial\left(C_Q/\sigma\right)}{\partial\theta}\right]_{\text{const. } \alpha}$ in autorotation.- For purposes of a subsequent

discussion, $\left[\dfrac{\partial\left(C_Q/\sigma\right)}{\partial\theta}\right]_{\text{const. } \alpha}$ for the sample helicopter in autorotation

is now obtained. For $\mu = 0.20$, $\dfrac{C_T}{\sigma} = 0.094$ but $\dfrac{P}{L} = 0$, interpolation

between the charts for $\theta = 4°$ and $\theta = 6°$ gives

$$\theta = 5.6°$$

$$\frac{\partial(P/L)}{\partial\left(C_T/\sigma\right)} = -4.4$$

$$\left[\frac{\partial(P/L)}{\partial\theta}\right]_{\text{const. } C_T/\sigma} = 3.1 \text{ per radian}$$

Thus, substitution in equation (20) yields

$$\left[\frac{\partial(C_Q/\sigma)}{\partial\theta}\right]_{const.\ \alpha} = 0.20(0.76)\left[0 + 0.094(-4.4)\right] + 0.20(0.094)(3.1)$$

$$= -0.063 + 0.058$$

$$= -0.005 \text{ per radian}$$

ROTOR STABILITY CHARACTERISTICS

Many significant stability characteristics of the helicopter rotor may be deduced from the charts presented herein. A number of these characteristics are now discussed. As further illustrations of the use of the charts, a number of specific stability problems and current suggestions as to means for improving helicopter stability are also discussed.

Rotor-Thrust Variations; Load Factors

Examination of figure 1(a) shows that the variation of $\dfrac{\partial(C_T/\sigma)}{\partial\alpha}$ with μ is approximately linear (about 1.2 power). Because (at constant rotational speed) rotor thrust is proportional to C_T and forward speed is proportional to μ, the load-factor increase per degree rotor angle-of-attack change also increases in approximately linear fashion with velocity. This result is in contrast with the variation with V^2 which applies for the airplane. Also, because a fixed gust velocity results in progressively lower angle-of-attack changes for increasing forward speeds, a sharp-edged gust of fixed velocity tends to produce about the same normal acceleration for all airspeeds, in contrast with a linear increase with airspeed for the airplane.

Figure 1(a) also shows that while $\dfrac{\partial(C_T/\sigma)}{\partial\theta}$ is much less affected by μ than is $\dfrac{\partial(C_T/\sigma)}{\partial\alpha}$, an appreciable increase does occur with increasing μ. A change in μ from 0.15 to 0.50 increases $\dfrac{\partial(C_T/\sigma)}{\partial\theta}$ about 50 percent. Thus, for a sudden increase in collective pitch, the increment in thrust per degree pitch increase at $\mu = 0.50$ is about 50 percent greater than that for $\mu = 0.15$.

Rotor Longitudinal Stability Characteristics; Variations of a'

For purposes of this discussion, the following assumptions are made:

(1) The helicopter being considered is a single-rotor machine with flapping hinges on the rotor shaft; therefore, its rotor force vector passes through its rotor hub.

(2) The helicopter center of gravity is in its normal position below the rotor hub and lies on the trim position of the rotor resultant-force vector.

For these conditions, pitching moments about the helicopter center of gravity depend primarily upon variations in a' and an increase in a' always causes a nose-up moment. (For those cases where the center of gravity is offset from the trim position of the rotor force vector, thrust variations produce additional pitching moments. Offset flapping hinges also result in additional pitching moments when there is longitudinal rotor blade flapping with respect to the rotor shaft.)

Power-on flight; variations of a' with angle of attack.- The charts of figure 3 indicate that, during power-on flight ($\theta = 4°$ to $14°$), the helicopter rotor is statically unstable with changes in angle of attack (or C_T/σ) at constant pitch, rotor speed, and forward speed. This instability can be deduced from the positive slope of the lines for constant tip-speed ratio. When the helicopter noses up, α increases and thus C_T/σ increases. Inasmuch as the slope of the lines for constant μ is positive, an increase in a' results. Because a' is positive when the rotor force vector is tilted behind the axis of no feathering, an increase in a' (with no change in longitudinal stick position) results in a nose-up pitching moment on the helicopter; therefore, the rotor is statically unstable with change in angle of attack at constant pitch, rotor speed, and forward speed.

Comparison of the slopes of the various lines for constant μ shows that $\dfrac{\partial a'}{\partial(C_T/\sigma)}$ increases (that is, becomes more unstable) approximately linearly with increasing μ at constant C_T/σ and θ. Thus, inasmuch as $\dfrac{\partial(C_T/\sigma)}{\partial\alpha}$ varies approximately with $\mu^{1.2}$, $\partial a'/\partial\alpha$ varies approximately with $\mu^{2.2}$ at constant C_T/σ and θ. Comparison of the various charts of figure 3 reveals that the rotor instability with angle of attack increases with increasing θ and, therefore, in general, with increasing rotor-shaft power. This increase in instability can be deduced from the increasing slope of the lines for constant μ with increasing θ. Thus,

the variation of $\partial a'/\partial \alpha$ with increases in level-flight forward speed
(beyond the speed for minimum power) has an exponent even higher
than 2.2 because of the increase in θ with increase in level-flight
speed. The increase in thrust that accompanies an increase in angle of
attack further adds to the rotor static instability. (See reference 11.)
The rapid increase in instability at the higher forward speeds as shown
experimentally in figure 4 of reference 2 is thus seen to be explainable
by means of these charts.

Methods for offsetting unstable variation of a' with angle of
attack.- Inasmuch as the helicopter rotor is statically unstable with
angle of attack in forward flight, some means must be incorporated on
the helicopter to offset this characteristic. One means is to use a
horizontal tail surface as discussed in references 3 and 11. By use of
the charts presented herein, the unstable rotor pitching moment per degree
change in angle of attack can be obtained and used to determine the size
of tail surface needed to stabilize the helicopter. Another method
which has received attention is to design the hub linkage in such a way as
to cause the collective pitch to decrease with increasing coning angle.
Theory indicates that a_1 decreases with decreasing collective pitch at
constant C_T/σ and μ. (See fig. 4.) As a result, when a_1 is assumed
equal to a', analysis indicates that a helicopter rotor with sufficient
"pitch-cone" change would be stable with angle of attack at constant rota-
tional speed, forward speed, and collective-pitch lever position.

By means of the charts of figure 3, this method may be examined with-
out relying on the assumption that a_1 is equal to a'. Comparison of the
various charts of figure 3 shows that, for typical cruising conditions for
current helicopters, improvements in stability should be obtainable.
Further comparison shows, however, that a', unlike a_1 does not neces-
sarily decrease with decreasing pitch at constant C_T/σ and μ and
that at high values of the ratio $\dfrac{\theta}{C_T/\sigma}$, a' actually increases with
decreasing pitch. Under these circumstances, if a given angle-of-attack
change is considered, then the pitch-cone change will, by minimizing the
increase in rotor thrust (and, therefore, C_T/σ), reduce the increase in a'
caused by the increased rotor angle of attack. The pitch-cone change can-
not, however, result in stable moments because some increase in thrust
must be permitted. Also, if a given increase in thrust is required, as
for a specific maneuver, under these circumstances the result is a greater
unstable moment than without the pitch-cone change. The value of the
parameter $\dfrac{\theta}{C_T/\sigma}$, above which a' increases with decreasing pitch at
constant μ and C_T/σ, varies from about 3 at $\mu = 0.15$ to about $2\frac{1}{2}$
at $\mu = 0.50$. Because stability problems appear likely to be more acute

for high-speed (over 150 mph), high-powered helicopters, additional cal-culations were made to determine the probable values of $\dfrac{\theta}{C_T/\sigma}$ for such designs. It was found that such helicopters, if of conventional basic design, will necessarily operate at values of $\dfrac{\theta}{C_T/\sigma}$ higher than 3; therefore, the preceding discussion appears applicable to this type of helicopter.

Power-on flight; variations of a' with speed.- The charts also reveal that, during power-on flight, the rotor is normally statically stable with variations in speed at constant pitch, rotor speed, and thrust. This stability is indicated by the increase in a' with increasing μ at constant C_T/σ. Thus, an increase in forward speed results in a rearward tilt of the rotor resultant force, tending to oppose the increase in speed. This tilt is, by definition, a stable variation; therefore, the rotor is statically stable with changes in speed. The spacing of the lines for constant μ indicates that the stability with speed is approximately constant for various speeds at constant C_T/σ and θ. However, at very low values of C_T/σ and high values of μ, for values of θ of 6° and higher, the charts indicate that the rotor becomes unstable with speed at constant C_T/σ. This instability indicates a problem for the high-speed helicopter, which will necessarily operate at low values of C_T/σ in order to avoid stalling.

Power-off flight; variations of a' with speed.- For power-off flight, the rotor speed varies during a gradual change in flight condition in such a way as to maintain zero aerodynamic torque; although for rapid changes in flight condition, rotor inertia prevents the rotor from reaching its equilibrium speed for a significant amount of time. The derivatives for slow changes in flight condition are thus obtained by following the lines for $\dfrac{P}{L} = 0$. For values of $\theta \geqq 2°$, the autorotating rotor is, unlike the power-on case, neutrally stable with speed at constant angle of attack. (The case of 0° pitch is discussed subsequently.) This statement can be understood when it is realized that at $\dfrac{P}{L} = 0$ and constant θ and α, μ and, therefore, a' must remain constant. (One point on the charts represents the whole speed range.) The physical meaning is that a slow variation in forward speed at constant angle of attack results in a pro-portional variation in rotor speed, such that the tip-speed ratio and, therefore, a' remain constant. Thus, the stability with speed at con-stant α is neutral. Inasmuch as C_T/σ also remains constant during a variation in forward speed at constant α, the accompanying variation in rotor speed results in a variation in magnitude of the rotor force. If

α $\left(\text{and because } \dfrac{\partial\left(C_T/\sigma\right)}{\partial\alpha} \text{ is always positive, } C_T/\sigma\right)$ is reduced with increase in forward speed in order to maintain constant thrust (as would be done in flight in order to maintain 1 g normal acceleration), the rotor speed increases less than in proportion to the forward speed. Thus, μ and a' increase and the rotor is stable with speed. These statements can be verified by noting that a reduction in C_T/σ along a line for $\dfrac{P}{L} = 0$ results in an increase in a' and an increase in μ. Thus, the autorotating rotor at constant thrust is stable with speed as for the power-on case; whereas at constant α it has neutral stability with speed.

It might be pointed out that the fixed-wing airplane has these same two types of stability with speed. If Mach number and power effects are ignored, the fixed-wing airplane has neutral stability with speed at constant angle of attack and is stable with speed at constant lift.

Power-off flight; variations of a' with angle of attack.- For the same pitch range, the autorotating rotor is, in contrast to the power-on case, statically stable with angle of attack $\left(\text{or } C_T/\sigma\right)$ at constant forward speed. This statement can be deduced by again examining the lines for $\dfrac{P}{L} = 0$. An increase in α results in an increase in C_T/σ and therefore a reduction in μ and a' because the lines for $\dfrac{P}{L} = 0$ slope down to the right. The physical meaning is that, if α is slowly increased, the rotor speed will increase and μ will be reduced at constant forward speed. Owing to the stability with changes in tip-speed ratio, the reduction in μ produces a decrease in a' which overcomes the increase in a' due to the increase in α at constant μ $\left(\text{near } \dfrac{P}{L} = 0\right)$, and thus a' is reduced. Thus, because the rotor speed varies during a slow change in α, the autorotating rotor is stable with slow changes in angle of attack.

Power-off flight; $\theta = 0°$.- For the case of $\theta = 0°$, the same ideas about variations in a' with speed and angle of attack apply as for the higher pitch values except that the variation of C_T/σ with μ (and α) is negligible.

Rotor-speed effect; power-on flight.- A rotor-speed effect occurs in power-on flight similar to that in autorotation in that if α is slowly increased, the rotor speed (and engine speed) will increase somewhat due to the reduction in C_Q/σ (at constant μ). The resulting reduction in μ reduces somewhat the rotor instability with angle of attack.

Variations of longitudinal stick position for trim.- These ideas
on the variation of a' with speed and angle of attack can be applied
directly to variations of helicopter longitudinal-control position
during steady unyawed flight if it is realized that longitudinal cyclic
pitch is equal to a' when the flapping hinges and the center of gravity
are on the rotor shaft and when fuselage pitching moments are negligible.

Rotor-Torque Variations

The variation of C_Q/σ with θ at constant μ and α is a sig-
nificant derivative for the coaxial helicopter which uses differential
torque obtained by differential collective pitch for yawing control.
The sample calculations of the previous section confirm results, which
are understood to have been obtained in flight tests, indicating that
this means of yawing control involves large variations in effectiveness
with changes in power. For the sample helicopter in autorotation at
$\mu = 0.20$ and $\dfrac{C_T}{\sigma} = 0.094$, the variation of C_Q/σ with θ at constant μ
and α is about 20 percent of the level-flight value and is reversed
in sign. Thus, a coaxial helicopter relying solely on this type of
control would have reversed yawing control at this flight condition.
At some intermediate power condition, the helicopter would have no
yawing control. Thus, coaxial helicopters apparently must use some
additional source of yawing control in the low power and autorotative
conditions for satisfactory flying qualities. Synchropter-type heli-
copters that rely entirely on differential collective pitch for yaw
control are understood to have also encountered this large variation
in yawing control effectiveness.

CONCLUSIONS

Theoretically derived charts have been presented from which the
longitudinal-stability derivatives of a helicopter rotor in forward
flight (except those depending on pitching velocity) can be conveniently
calculated for tip-speed ratios from 0.15 to 0.50. Examination of
several basic or current problems by means of these charts indicated the
following conclusions:

1. Comparison between theoretical values of rates of change of a'
(longitudinal angle between the rotor force vector and axis of no
feathering) and a_1 (longitudinal flapping coefficient) in general
shows large differences. Thus, the use of the assumption that the rotor
force vector is perpendicular to the tip-path plane and, therefore, that
$a_1 = a'$ (often resorted to for convenience) can lead to large errors in
stability calculations.

2. The load-factor increase per degree rotor angle-of-attack change (at constant rotational speed) increases in approximately linear fashion with the forward velocity V. This result is in contrast with the variation with V^2 which applies for the airplane.

3. In power-on flight, the rotor is unstable with angle of attack and is ordinarily statically stable with speed. The instability with angle of attack increases with increasing trim value of tip-speed ratio or of power setting but is reduced somewhat if the rotor speed varies due to the accompanying change in aerodynamic torque.

4. The autorotating rotor is neutrally stable with speed at constant angle of attack, is stable with speed at constant thrust, and is also stable with slow change in angle of attack at constant forward speed. The autorotating rotor is different from the powered rotor because of the rotor rotational-speed variation with slow change in flight condition.

5. The charts confirm the reduction or reversal of yawing control which is understood to be encountered in low-powered flight and auto-rotation in coaxial and synchropter-type helicopters when differential torque, as obtained by means of differential collective pitch, is employed as the only source of yawing control.

Langley Aeronautical Laboratory
    National Advisory Committee for Aeronautics
        Langley Field, Va., November 25, 1950

APPENDIX A

DERIVATIONS OF C_T/σ DERIVATIVES

By combining equations (6) and (7) of reference 4, the following equation is obtained (omitting the blade-twist term):

$$\frac{C_T}{\sigma}\left[\frac{\sigma t_{3,1}}{2\mu\sqrt{1 + \left(\dfrac{\lambda}{\mu}\right)^2}} + \frac{2}{a}\right] = t_{3,1}\mu\tan\alpha + t_{3,2}\theta \tag{A1}$$

Derivative of C_T/σ with respect to θ.- Differentiation of equation (A1) with respect to θ at constant μ and α yields the following equation:

$$\frac{\partial(C_T/\sigma)}{\partial\theta}\left[\frac{\sigma t_{3,1}}{2\mu\sqrt{1 + \left(\dfrac{\lambda}{\mu}\right)^2}} + \frac{2}{a}\right] + \frac{C_T}{\sigma}\left\{-\frac{\sigma t_{3,1}\dfrac{\lambda}{\mu}\dfrac{\partial(\lambda/\mu)}{\partial\theta}}{2\mu\left[1 + \left(\dfrac{\lambda}{\mu}\right)^2\right]^{3/2}}\right\} = t_{3,2} \tag{A2}$$

but

$$\frac{\partial(\lambda/\mu)}{\partial\theta} = \frac{\partial(\lambda/\mu)}{\partial(C_T/\sigma)}\frac{\partial(C_T/\sigma)}{\partial\theta} \tag{A3}$$

Substituting for $\dfrac{\partial(\lambda/\mu)}{\partial\theta}$ in equation (A2) and combining terms gives

$$\frac{\partial(C_T/\sigma)}{\partial\theta}\left\{\frac{2}{a} + \frac{\sigma t_{3,1}}{2\mu\sqrt{1 + \left(\dfrac{\lambda}{\mu}\right)^2}}\left[1 - \frac{\dfrac{\lambda}{\mu}\dfrac{C_T}{\sigma}\dfrac{\partial(\lambda/\mu)}{\partial(C_T/\sigma)}}{1 + \left(\dfrac{\lambda}{\mu}\right)^2}\right]\right\} = t_{3,2} \tag{A4}$$

Thus,

$$\frac{\partial(C_T/\sigma)}{\partial\theta} = \frac{t_{3,2}}{\frac{2}{a} + \frac{t_{3,1}\sigma C}{2\mu}} \qquad (A5)$$

where

$$C = \frac{1 - \dfrac{\dfrac{\lambda}{\mu}\dfrac{C_T}{\sigma}\dfrac{\partial(\lambda/\mu)}{\partial(C_T/\sigma)}}{1 + \left(\dfrac{\lambda}{\mu}\right)^2}}{\sqrt{1 + \left(\dfrac{\lambda}{\mu}\right)^2}} \qquad (A6)$$

The expression for C can be reduced to a more convenient form as follows:
Equation (7) of reference 4 can be rewritten as

$$\frac{\lambda}{\mu} = \tan\alpha - \frac{C_T}{2\mu^2\sqrt{1 + \left(\dfrac{\lambda}{\mu}\right)^2}}$$

Differentiating with respect to C_T/σ at constant μ and α gives

$$\frac{\partial(\lambda/\mu)}{\partial(C_T/\sigma)} = 0 - \frac{1}{\frac{2\mu^2}{\sigma}\sqrt{1 + \left(\dfrac{\lambda}{\mu}\right)^2}} + \frac{C_T\dfrac{\lambda}{\mu}\dfrac{\partial(\lambda/\mu)}{\partial(C_T/\sigma)}}{2\mu^2\left[1 + \left(\dfrac{\lambda}{\mu}\right)^2\right]^{3/2}} \qquad (A7)$$

Rearranging terms gives

$$\frac{\partial(\lambda/\mu)}{\partial(C_T/\sigma)}\left\{1 - \frac{C_T}{2\mu^2}\frac{\lambda/\mu}{\left[1 + \left(\dfrac{\lambda}{\mu}\right)^2\right]^{3/2}}\right\} = -\frac{1}{\frac{2\mu^2}{\sigma}\sqrt{1 + \left(\dfrac{\lambda}{\mu}\right)^2}} \qquad (A8)$$

Thus,

$$\frac{\partial(\lambda/\mu)}{\partial\left(C_T/\sigma\right)} = - \cfrac{1}{\cfrac{2\mu^2}{\sigma}\sqrt{1 + \left(\cfrac{\lambda}{\mu}\right)^2} - \cfrac{\cfrac{C_T}{\sigma}\cfrac{\lambda}{\mu}}{1 + \left(\cfrac{\lambda}{\mu}\right)^2}} \qquad (A9)$$

Combining equations (A6) and (A9) gives

$$C = \cfrac{1 + \cfrac{1}{\cfrac{2\mu^2}{C_T}\cfrac{\left[1 + (\lambda/\mu)^2\right]^{3/2}}{\lambda/\mu} - 1}}{\sqrt{1 + \left(\cfrac{\lambda}{\mu}\right)^2}} \qquad (A10)$$

Calculations indicate that, for $\mu \geqq 0.15$, the parameter C is relatively independent of variations in λ and C_T and thus depends primarily upon μ. Hence, inasmuch as $t_{3,1}$ and $t_{3,2}$ depend upon μ only, equation (A5) indicates that $\dfrac{\partial\left(C_T/\sigma\right)}{\partial\theta}$ is primarily a function of μ and σ. Thus, the values of $\dfrac{\partial\left(C_T/\sigma\right)}{\partial\theta}$ plotted in figure 1(a), which were calculated using $\lambda = -0.05$ and $C_T = 0.005$, are less than 4 percent in error for λ between 0.05 and -0.10 and C_T between 0.002 and 0.008.

Derivative of C_T/σ with respect to α.- Differentiation of equation (A1) with respect to α at constant μ and θ and repeating the procedure of the previous section yields the following equation:

$$\frac{\partial\left(C_T/\sigma\right)}{\partial\alpha} = \frac{t_{3,1}\mu}{\cos^2\alpha\left(\dfrac{2}{a} + \dfrac{t_{3,1}\sigma C}{2\mu}\right)} \qquad (A11)$$

where C is given by equation (A10). As mentioned previously, C is primarily a function of μ for $\mu \geqq 0.15$. For values of α less than $10°$ in magnitude $\cos^2\alpha$ can be assumed equal to unity with no more than a 3-percent error. Thus, for $\mu \geqq 0.15$, $\dfrac{\partial\left(C_T/\sigma\right)}{\partial\alpha}$ is primarily a function of μ and σ. Thus, the values of $\dfrac{\partial\left(C_T/\sigma\right)}{\partial\alpha}$ plotted in figure 1(a), which

were calculated using $\lambda = -0.05$, $C_T = 0.005$, and $\alpha = 0$, are less than 7 percent in error for λ between 0.05 and -0.10, C_T between 0.002 and 0.008, and α less than $10°$ in magnitude.

Derivative of C_T/σ with respect to μ.- The derivative of C_T/σ with respect to μ at constant α and θ can be set up conveniently as follows:

$$\left[\frac{\partial(C_T/\sigma)}{\partial\mu}\right]_{\text{const. }\alpha,\theta} = \left[\frac{\partial(C_T/\sigma)}{\partial\mu}\right]_{\text{const. }\lambda,\theta} - \frac{\partial(C_T/\sigma)}{\partial\alpha}\left(\frac{\partial\alpha}{\partial\mu}\right)_{\text{const. }\lambda,\theta} \qquad (A12)$$

Differentiation of equations (6) and (7) of reference 4 with respect to μ at constant λ and θ results in the following equation (omitting the blade-twist term):

$$\left[\frac{\partial(C_T/\sigma)}{\partial\mu}\right]_{\text{const. }\lambda,\theta} = \frac{a}{2}\left(\lambda\,\frac{\partial t_{3,1}}{\partial\mu} + \theta\,\frac{\partial t_{3,2}}{\partial\mu}\right) \qquad (A13)$$

$$\left(\frac{\partial\alpha}{\partial\mu}\right)_{\text{const. }\lambda,\theta} = \cos^2\alpha\left[-\frac{\lambda}{\mu^2} - \frac{C_T}{2\mu^2\sqrt{\mu^2 + \lambda^2}} - \frac{C_T}{2(\lambda^2 + \mu^2)^{3/2}}\right] \qquad (A14)$$

Substitution of equations (A11), (A13), and (A14) in equation (A12) and rearrangement of terms yields the following equation:

$$\left[\frac{\partial(C_T/\sigma)}{\partial\mu}\right]_{\text{const. }\alpha,\theta} = \frac{a}{2}\left(\lambda\,\frac{\partial t_{3,1}}{\partial\mu} + \theta\,\frac{\partial t_{3,2}}{\partial\mu}\right) +$$

$$\left(\frac{t_{3,1}\mu}{\dfrac{2}{a} + \dfrac{t_{3,1}\sigma C}{2\mu}}\right)\left\{\frac{\lambda}{\mu^2} + \frac{C_T}{2\mu^3\sqrt{1 + \left(\dfrac{\lambda}{\mu}\right)^2}} + \frac{C_T}{2\mu^3\left[1 + \left(\dfrac{\lambda}{\mu}\right)^2\right]^{3/2}}\right\} \qquad (A15)$$

For normal values of λ/μ, the last two terms of the braced expression can be approximated satisfactorily by means of the binomial theorem as follows:

$$\frac{C_T}{2\mu^3}\left\{\frac{1}{\sqrt{1 + \left(\dfrac{\lambda}{\mu}\right)^2}} + \frac{1}{\left[1 + \left(\dfrac{\lambda}{\mu}\right)^2\right]^{3/2}}\right\} \approx \frac{C_T}{\mu^3}\left[1 - \left(\frac{\lambda}{\mu}\right)^2\right] \qquad (A16)$$

Substituting this approximate equation in equation (A15), expressing λ in terms of C_T and θ by means of equation (6) of reference 4, and rearranging terms results in the following equation for $\dfrac{\partial\left(C_T/\sigma\right)}{\partial\mu}$ at constant α and θ:

$$\frac{\partial\left(C_T/\sigma\right)}{\partial\mu} = k_1\theta + k_2\,\frac{C_T}{\sigma} + k_3 C_T\theta^2 + k_4\,\frac{C_T^2\theta}{\sigma} + k_5\,\frac{C_T^3}{\sigma^2} \qquad (A17)$$

where

$$k_1 = \frac{a}{2}\,\frac{\partial t_{3,2}}{\partial\mu} - \frac{a}{2}\,\frac{t_{3,2}}{t_{3,1}}\,\frac{\partial t_{3,1}}{\partial\mu} - \frac{t_{3,2}}{\mu\left(\dfrac{2}{a} + \dfrac{t_{3,1}\sigma C}{2\mu}\right)}$$

$$k_2 = \frac{1}{t_{3,1}}\,\frac{\partial t_{3,1}}{\partial\mu} + \frac{2}{a\mu\left(\dfrac{2}{a} + \dfrac{t_{3,1}\sigma C}{2\mu}\right)} + \frac{t_{3,1}\sigma}{\mu^2\left(\dfrac{2}{a} + \dfrac{t_{3,1}\sigma C}{2\mu}\right)}$$

$$k_3 = -\left(\frac{t_{3,2}}{t_{3,1}}\right)^2 \frac{t_{3,1}}{\mu^4\left(\dfrac{2}{a} + \dfrac{t_{3,1}\sigma C}{2\mu}\right)}$$

$$k_4 = \frac{4t_{3,2}}{at_{3,1}\mu^4\left(\dfrac{2}{a} + \dfrac{t_{3,1}\sigma C}{2\mu}\right)}$$

$$k_5 = -\frac{4}{a^2 t_{3,1}\mu^4\left(\dfrac{2}{a} + \dfrac{t_{3,1}\sigma C}{2\mu}\right)}$$

The parameter C is given by equation (A10).

Although, as discussed previously, the parameter C varies somewhat
with λ and C_T, calculations indicate that the values of k plotted in
figure 1(b) using λ = -0.05 and C_T = 0.005 are less than 4 percent in
error for values of λ between 0.05 and -0.10 and values of C_T between
0.002 and 0.008. Examination of equation (A16) indicates it to be suf-
ficiently accurate for values of λ/μ of smaller magnitude than 0.5. For
special cases with values of λ/μ larger in magnitude than 0.5, or with
values of C_T or λ outside the range for reasonable accuracy in the
values of k, equations (A10) and (A15) can be used.

APPENDIX B

SAMPLE DERIVATIONS OF EQUATIONS FOR USE WITH FIGURE 3

In the section entitled "Method of Obtaining Stability Derivatives," simple formulas are given for use in obtaining stability derivatives from figure 3. In this appendix, the most significant of these formulas are derived. The derivations of the remaining formulas are then readily deducible and consequently are not specifically discussed.

$\partial a'/\partial \alpha$ derivative.- If the rules for differentiation are followed, $\partial a'/\partial \alpha$ can be written as

$$\frac{\partial a'}{\partial \alpha} = \frac{\partial a'}{\partial \left(C_T/\sigma\right)} \frac{\partial \left(C_T/\sigma\right)}{\partial \alpha}$$

$\partial a'/\partial V$ derivative at constant C_T/σ.- As before, the rules for differentiation give

$$\left(\frac{\partial a'}{\partial V}\right)_{\text{const. } C_T/\sigma} = \frac{\partial \mu}{\partial V}\left(\frac{\partial a'}{\partial \mu}\right)_{\text{const. } C_T/\sigma} = \frac{1}{\Omega R}\left(\frac{\partial a'}{\partial \mu}\right)_{\text{const. } C_T/\sigma}$$

$\partial a'/\partial V$ derivative at constant α.- The derivative $\partial a'/\partial \mu$ at constant α is first obtained as follows:

$$\left(\frac{\partial a'}{\partial \mu}\right)_{\text{const. } \alpha} = \left(\frac{\partial a'}{\partial \mu}\right)_{\text{const. } C_T/\sigma} + \frac{\partial a'}{\partial \left(C_T/\sigma\right)} \frac{\partial \left(C_T/\sigma\right)}{\partial \mu}$$

The second term takes account of the effect of any change in C_T/σ that occurs when μ is changed while keeping α constant. Then, as before,

$$\left(\frac{\partial a'}{\partial V}\right)_{\text{const. } \alpha} = \frac{\partial \mu}{\partial V}\left(\frac{\partial a'}{\partial \mu}\right)_{\text{const. } \alpha} = \frac{1}{\Omega R}\left[\left(\frac{\partial a'}{\partial \mu}\right)_{\text{const. } C_T/\sigma} + \frac{\partial a'}{\partial \left(C_T/\sigma\right)} \frac{\partial \left(C_T/\sigma\right)}{\partial \mu}\right]$$

$\dfrac{\partial(C_Q/\sigma)}{\partial\alpha}$ derivative.- The coefficient C_Q/σ is given as a function

of P/L by the following expression from reference 5:

$$2\,\frac{C_Q}{\sigma} = \frac{P}{L}\,\frac{2C_T}{\sigma a}\,a\mu$$

Simplifying this equation gives

$$\frac{C_Q}{\sigma} = \frac{P}{L}\,\frac{C_T}{\sigma}\,\mu \tag{B1}$$

Differentiating equation (B1) gives

$$\frac{\partial(C_Q/\sigma)}{\partial\alpha} = \frac{P}{L}\,\mu\,\frac{\partial(C_T/\sigma)}{\partial\alpha} + \mu\,\frac{C_T}{\sigma}\,\frac{\partial(P/L)}{\partial\alpha}$$

However,

$$\frac{\partial(P/L)}{\partial\alpha} = \frac{\partial(P/L)}{\partial(C_T/\sigma)}\,\frac{\partial(C_T/\sigma)}{\partial\alpha}$$

Therefore,

$$\frac{\partial(C_Q/\sigma)}{\partial\alpha} = \mu\,\frac{\partial(C_T/\sigma)}{\partial\alpha}\left[\frac{P}{L} + \frac{C_T}{\sigma}\,\frac{\partial(P/L)}{\partial(C_T/\sigma)}\right]$$

$\dfrac{\partial(C_Q/\sigma)}{\partial\theta}$ derivative at constant C_T/σ.- Differentiation of equation (B1) with respect to θ at constant μ and C_T/σ yields

$$\left[\frac{\partial(C_Q/\sigma)}{\partial\theta}\right]_{\text{const. } C_T/\sigma} = \mu\,\frac{C_T}{\sigma}\left[\frac{\partial(P/L)}{\partial\theta}\right]_{\text{const. } C_T/\sigma}$$

$\dfrac{\partial(C_Q/\sigma)}{\partial\theta}$ derivative at constant α.- Differentiation of equation (B1) with respect to θ at constant μ and α yields

$$\left[\frac{\partial(C_Q/\sigma)}{\partial\theta}\right]_{\text{const. } \alpha} = \frac{P}{L}\,\mu\,\frac{\partial(C_T/\sigma)}{\partial\theta} + \mu\,\frac{C_T}{\sigma}\left[\frac{\partial(P/L)}{\partial\theta}\right]_{\text{const. } \alpha}$$

However,

$$\left[\frac{\partial(P/L)}{\partial\theta}\right]_{\text{const. } \alpha} = \left[\frac{\partial(P/L)}{\partial\theta}\right]_{\text{const. } C_T/\sigma} + \frac{\partial(P/L)}{\partial(C_T/\sigma)}\left[\frac{\partial(C_T/\sigma)}{\partial\theta}\right]_{\text{const. } \alpha}$$

The second term takes account of the effect of a variation in C_T/σ when θ is changed while keeping α constant. Thus,

$$\left[\frac{\partial(C_Q/\sigma)}{\partial\theta}\right]_{\text{const. } \alpha} = \mu\,\frac{\partial(C_T/\sigma)}{\partial\theta}\left[\frac{P}{L} + \frac{C_T}{\sigma}\,\frac{\partial(P/L)}{\partial(C_T/\sigma)}\right] + \mu\,\frac{C_T}{\sigma}\left[\frac{\partial(P/L)}{\partial\theta}\right]_{\text{const. } C_T/\sigma}$$

REFERENCES

1. Mazur, John W.: Flight Testing of Helicopters by the U. S. Navy.
   Proc. Fifth Annual Forum, Am. Helicopter Soc., Inc.,
   May 12, 13, 1949.

2. Reeder, John P., and Gustafson, F. B.: On the Flying Qualities of
   Helicopters. NACA TN 1799, 1949.

3. Gustafson, F. B., Amer, Kenneth B., Haig, C. R., and Reeder, J. P.:
   Longitudinal Flying Qualities of Several Single-Rotor Helicopters
   in Forward Flight. NACA TN 1983, 1949.

4. Bailey, F. J., Jr.: A Simplified Theoretical Method of Determining
   the Characteristics of a Lifting Rotor in Forward Flight. NACA
   Rep. 716, 1941.

5. Bailey, F. J., Jr., and Gustafson, F. B.: Charts for Estimation of
   the Characteristics of a Helicopter Rotor in Forward Flight. I –
   Profile Drag-Lift Ratio for Untwisted Rectangular Blades. NACA
   ACR L4H07, 1944.

6. Gustafson, F. B., and Gessow, Alfred: Analysis of Flight-Performance
   Measurements on a Twisted, Plywood-Covered Helicopter Rotor in
   Various Flight Conditions. NACA TN 1595, 1948.

7. Myers, Garry C., Jr.: Flight Measurements of Helicopter Blade Motion
   with a Comparison between Theoretical and Experimental Results.
   NACA TN 1266, 1947.

8. Amer, Kenneth B.: Theory of Helicopter Damping in Pitch or Roll and
   a Comparison with Flight Measurements. NACA TN 2136, 1950.

9. Tetervin, Neal: Airfoil Section Data from Tests of 10 Practical
   Construction Sections of Helicopter Rotor Blades Submitted by the
   Sikorsky Aircraft Division, United Aircraft Corporation. NACA MR,
   Sept. 6, 1944.

10. Wheatley, John B.: An Aerodynamic Analysis of the Autogiro Rotor
    with a Comparison between Calculated and Experimental Results.
    NACA Rep. 487, 1934.

11. Gessow, Alfred, and Amer, Kenneth B.: An Introduction to the Physical
    Aspects of Helicopter Stability. NACA TN 1982, 1949.
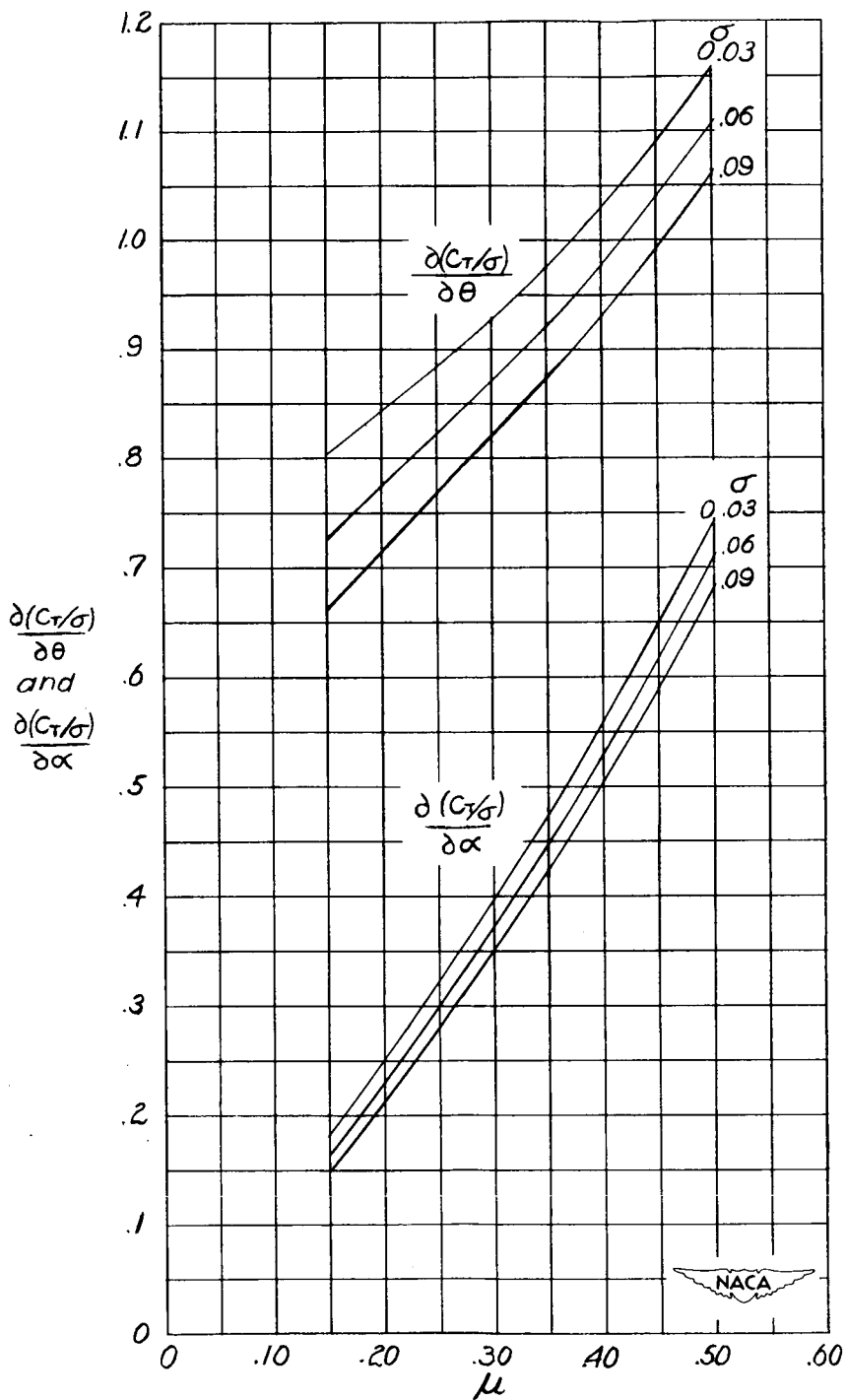
(a) $\dfrac{\partial\left(C_T/\sigma\right)}{\partial\alpha}$ and $\dfrac{\partial\left(C_T/\sigma\right)}{\partial\theta}$.

Figure 1.- C_T/σ derivatives.
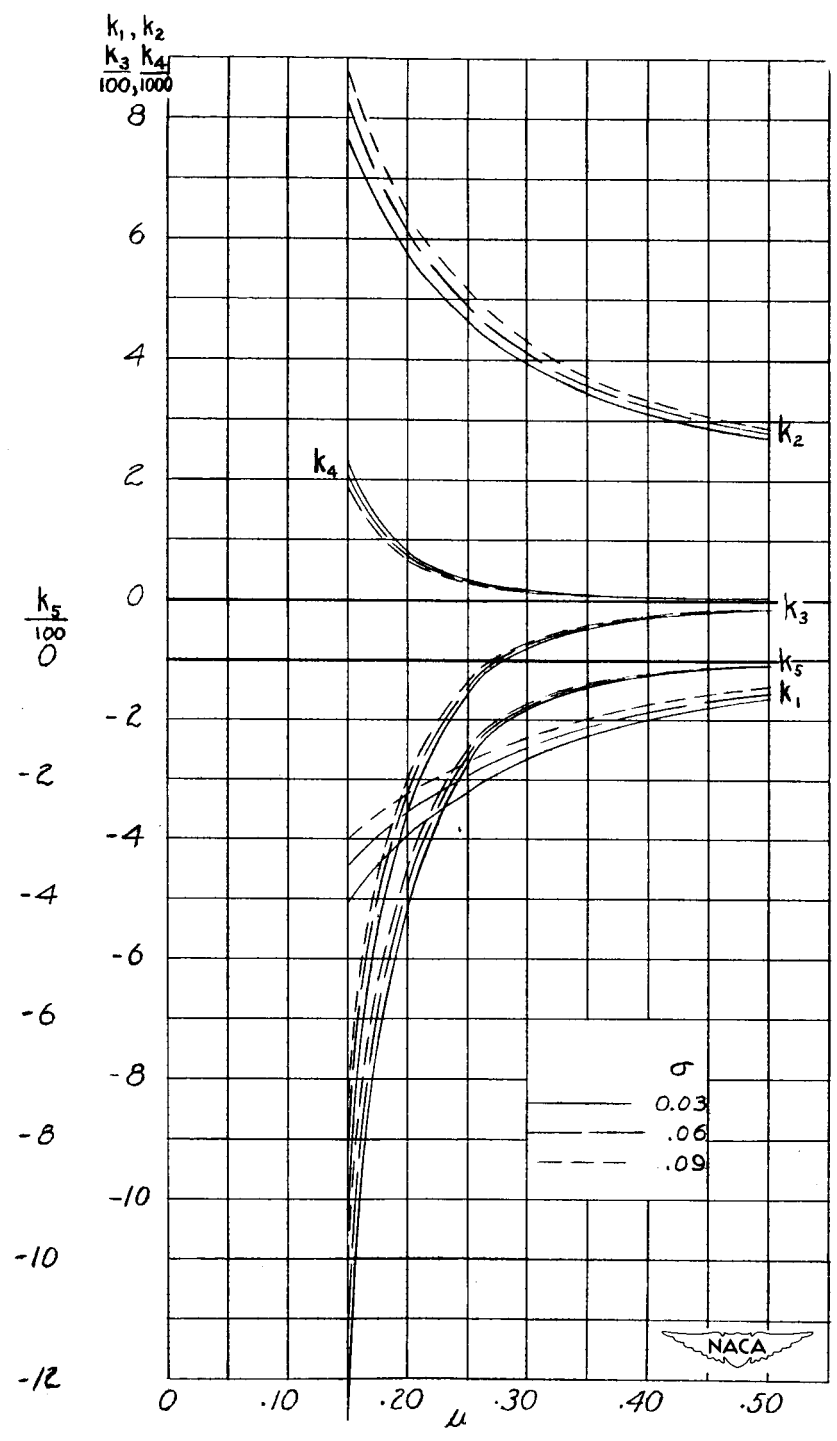
(b) $\dfrac{\partial\left(C_T/\sigma\right)}{\partial\mu} = k_1\theta + k_2\,\dfrac{C_T}{\sigma} + k_3 C_T\theta^2 + k_4\,\dfrac{C_T{}^2\theta}{\sigma} + k_5\,\dfrac{C_T{}^3}{\sigma^2}.$
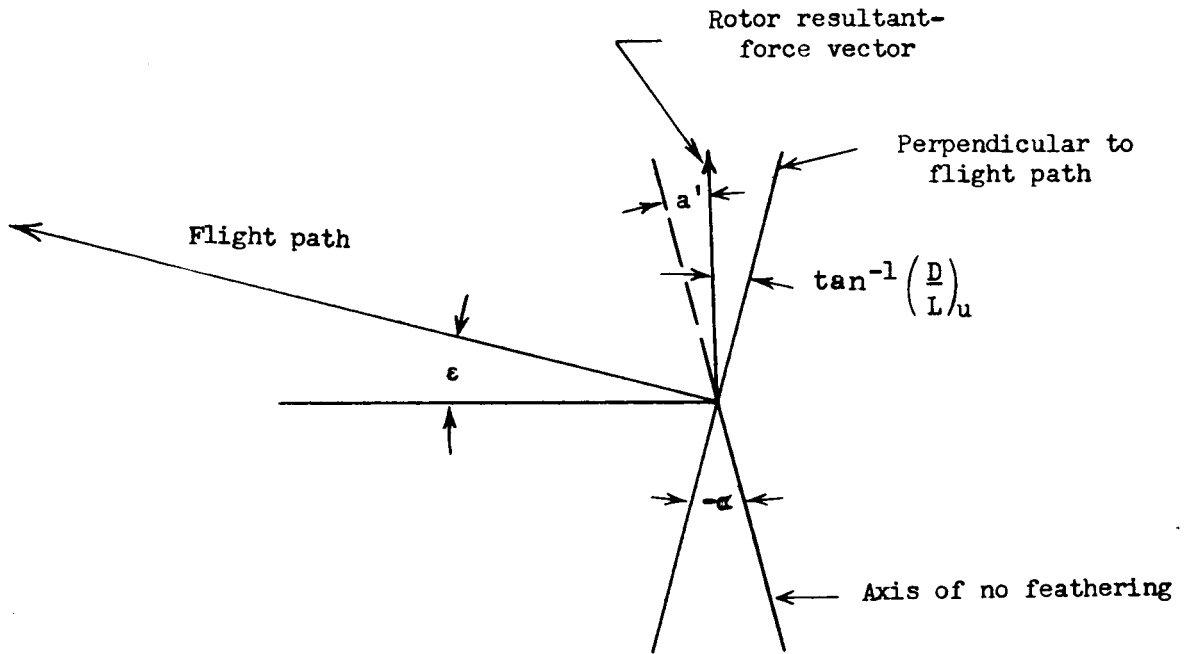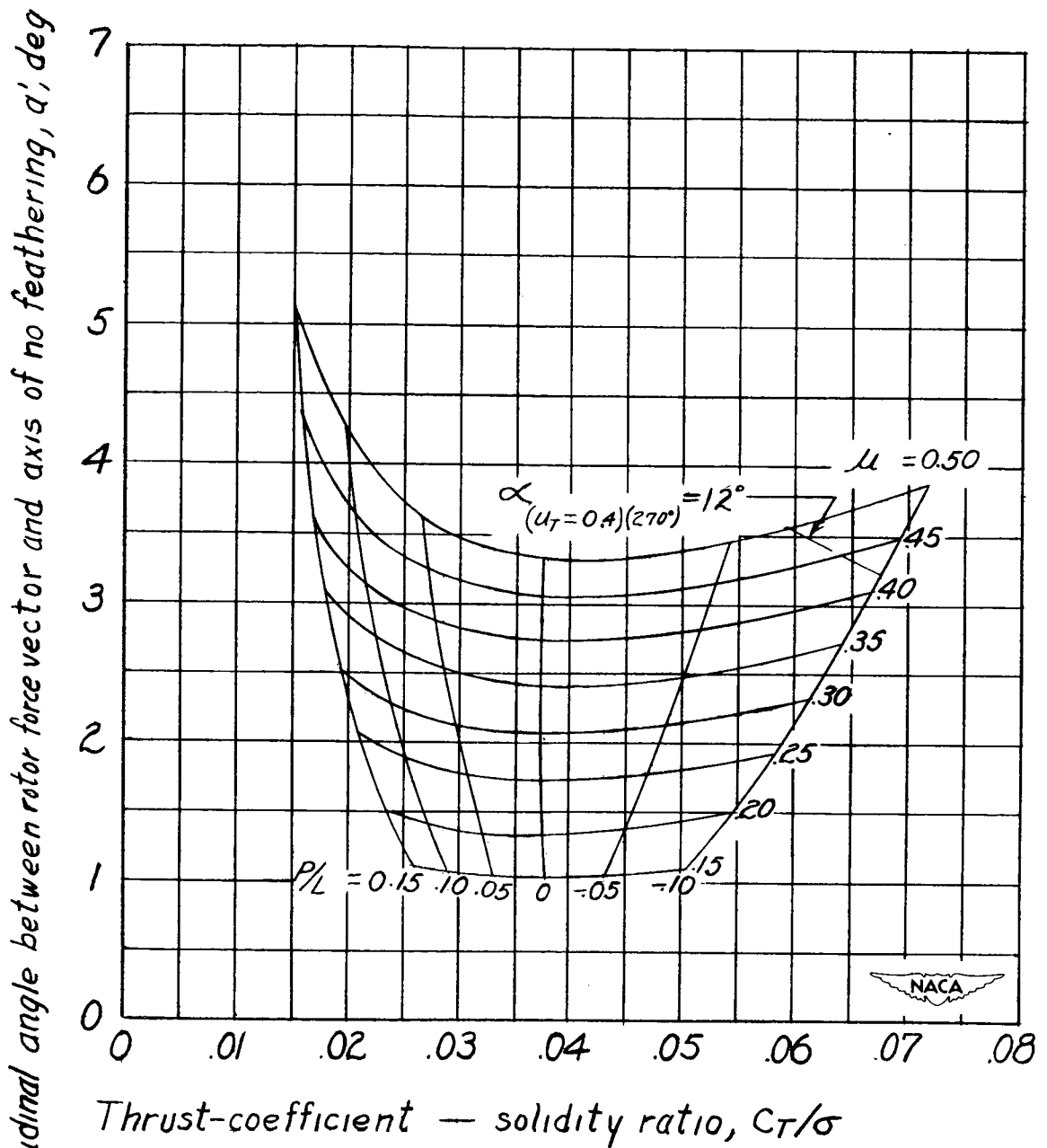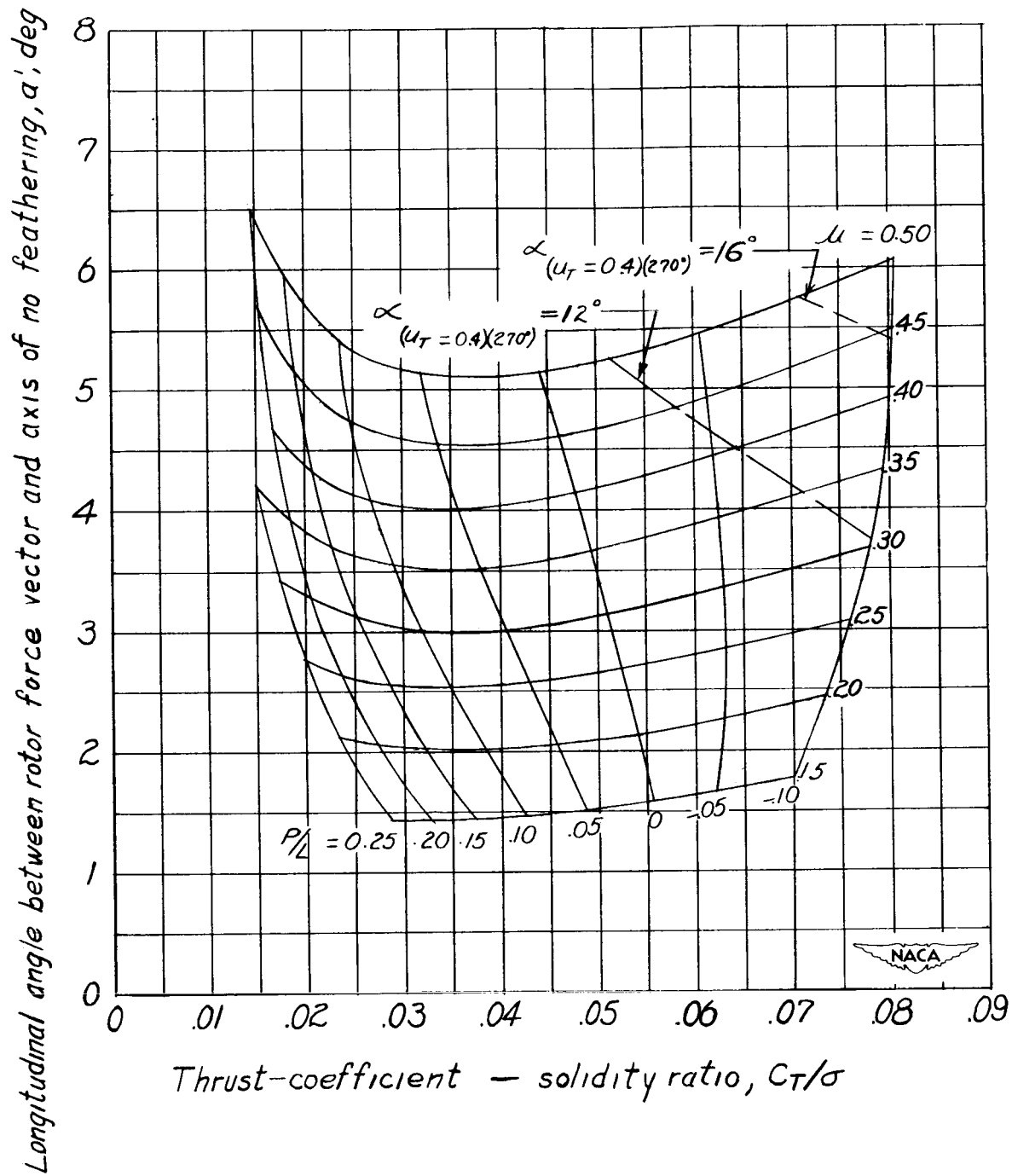
Figure 1.- Concluded.

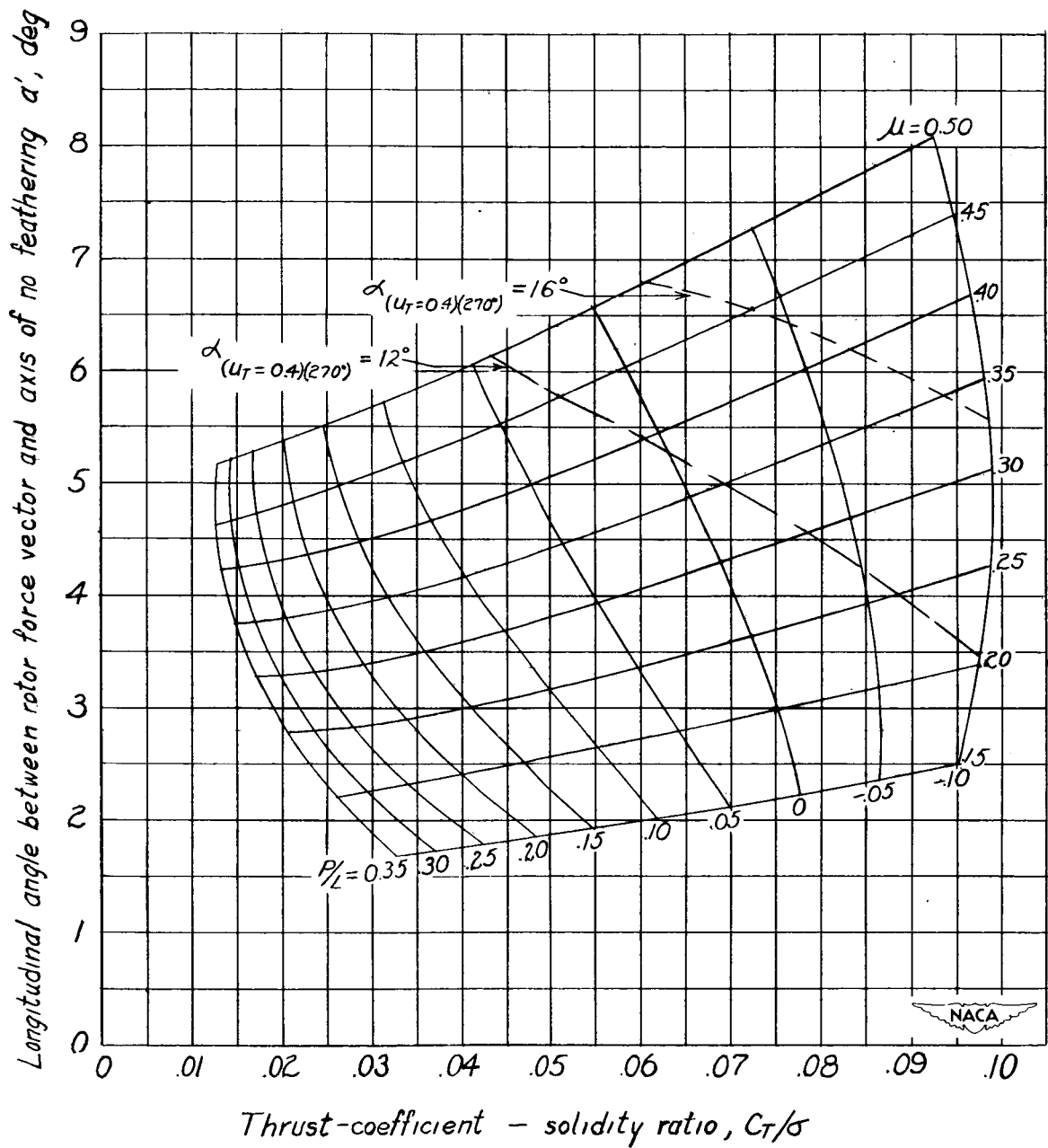Figure 2.- Schematic side view of helicopter rotor in forward flight.

(a) $\theta = 0^{\circ}$.

Figure 3.- Charts for determining a' and C_Q/σ derivatives.

(b) $\theta = 2°$.

Figure 3.- Continued.

(c) $\theta = 4^\circ$.

Figure 3.- Continued.
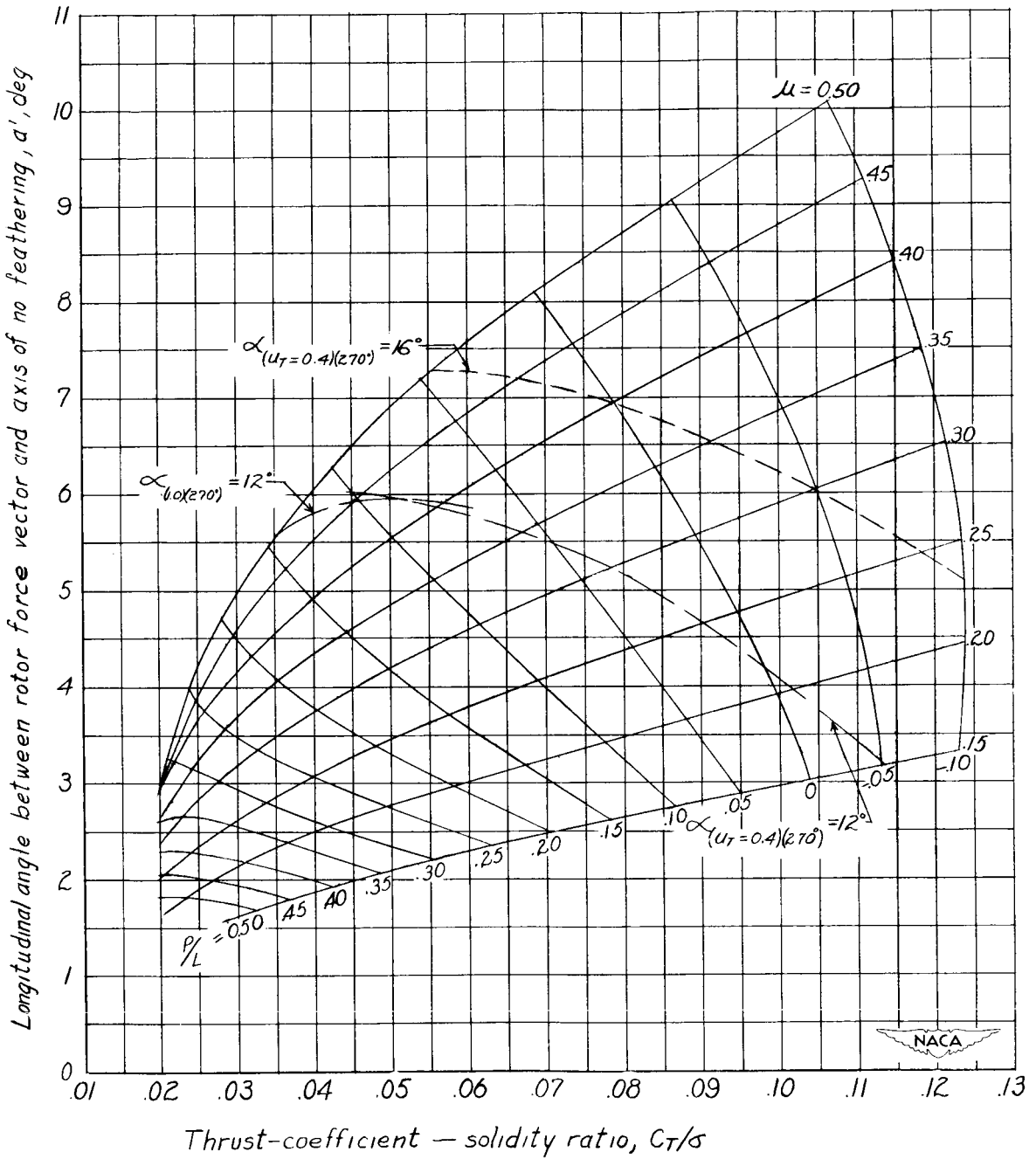
(d) $\theta = 6^{\circ}$.

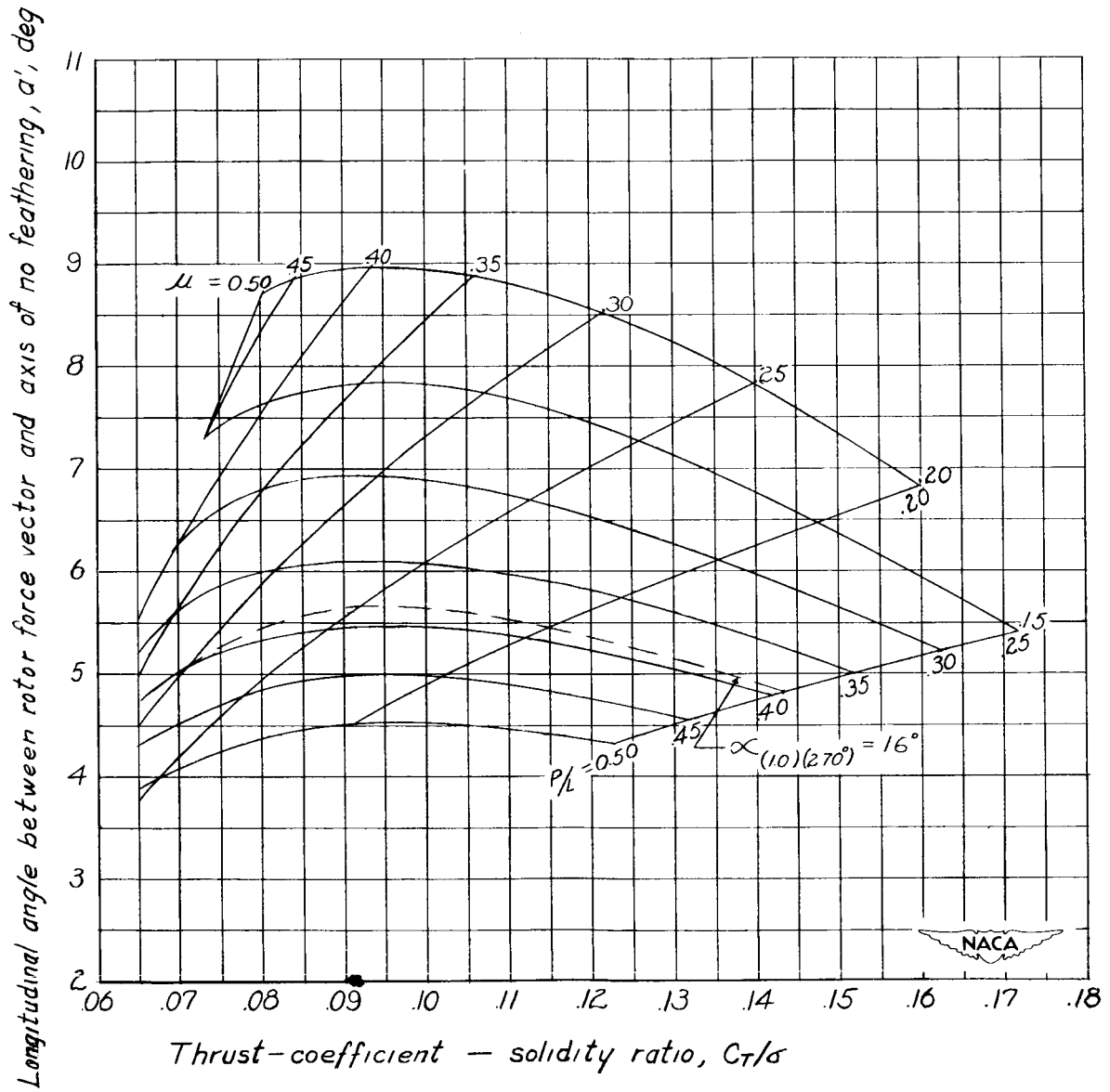Figure 3.- Continued.
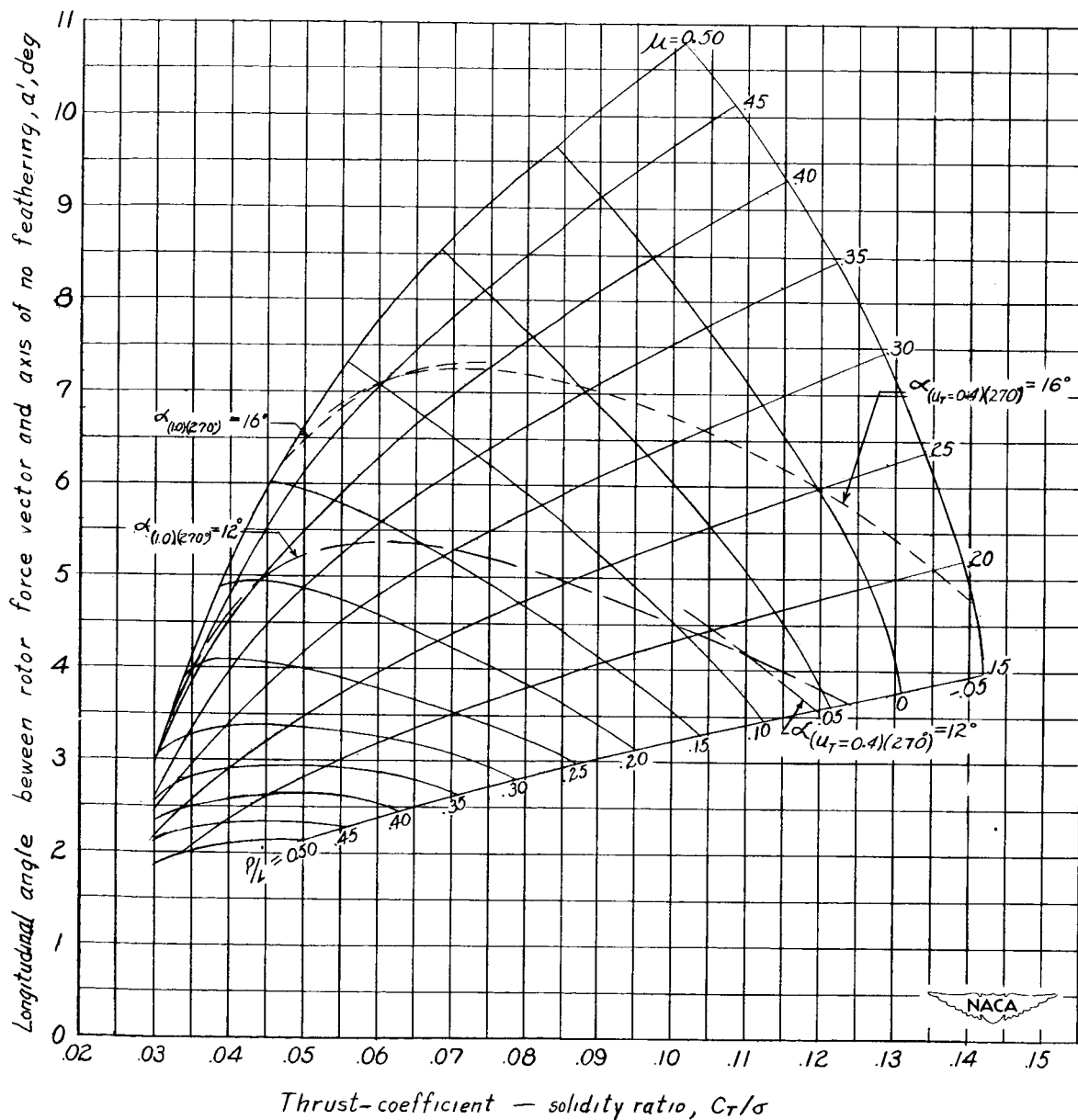
(e) $\theta = 8°$.

Figure 3.- Continued.
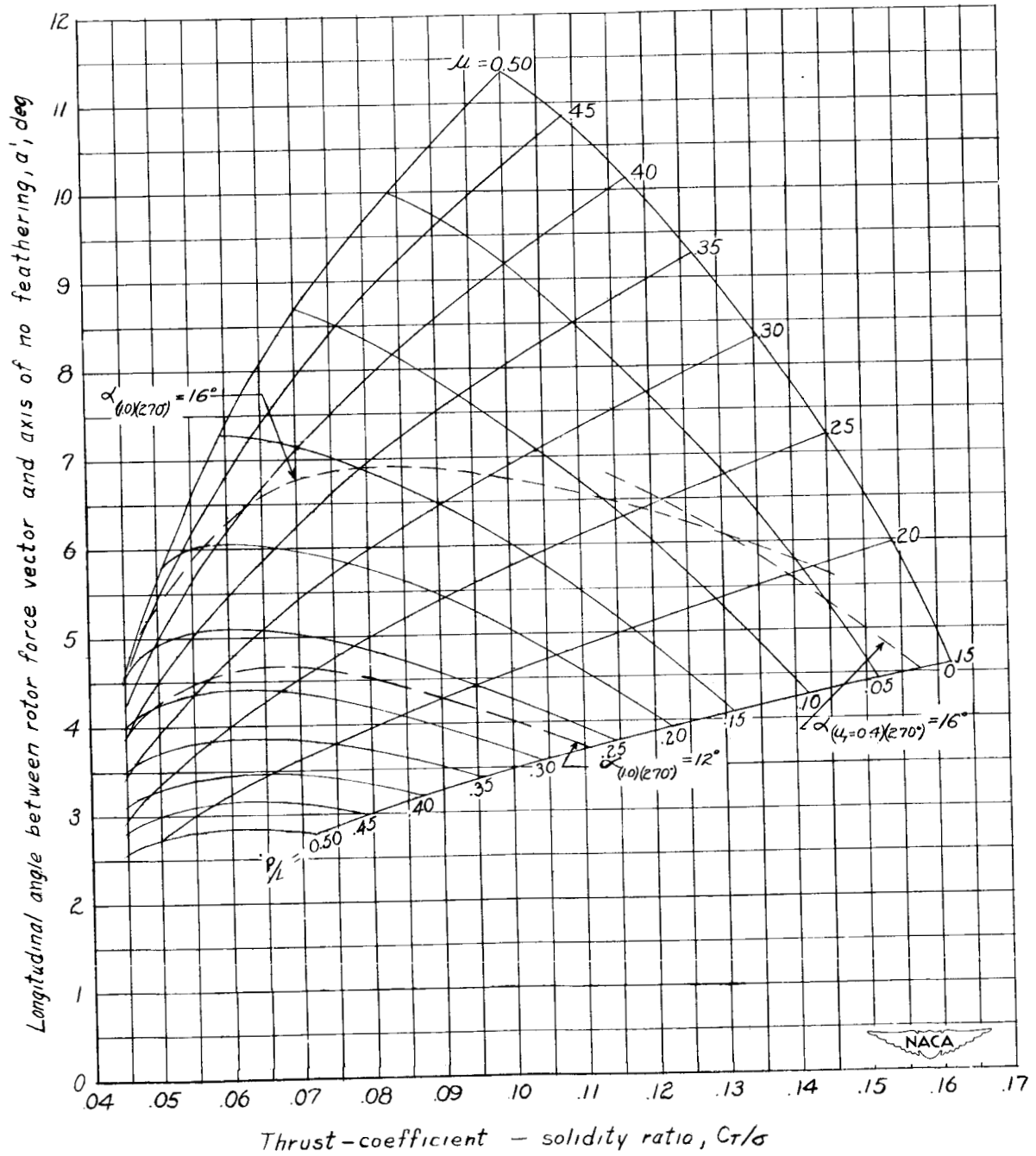
(f) $\theta = 10°$.

Figure 3.- Continued.
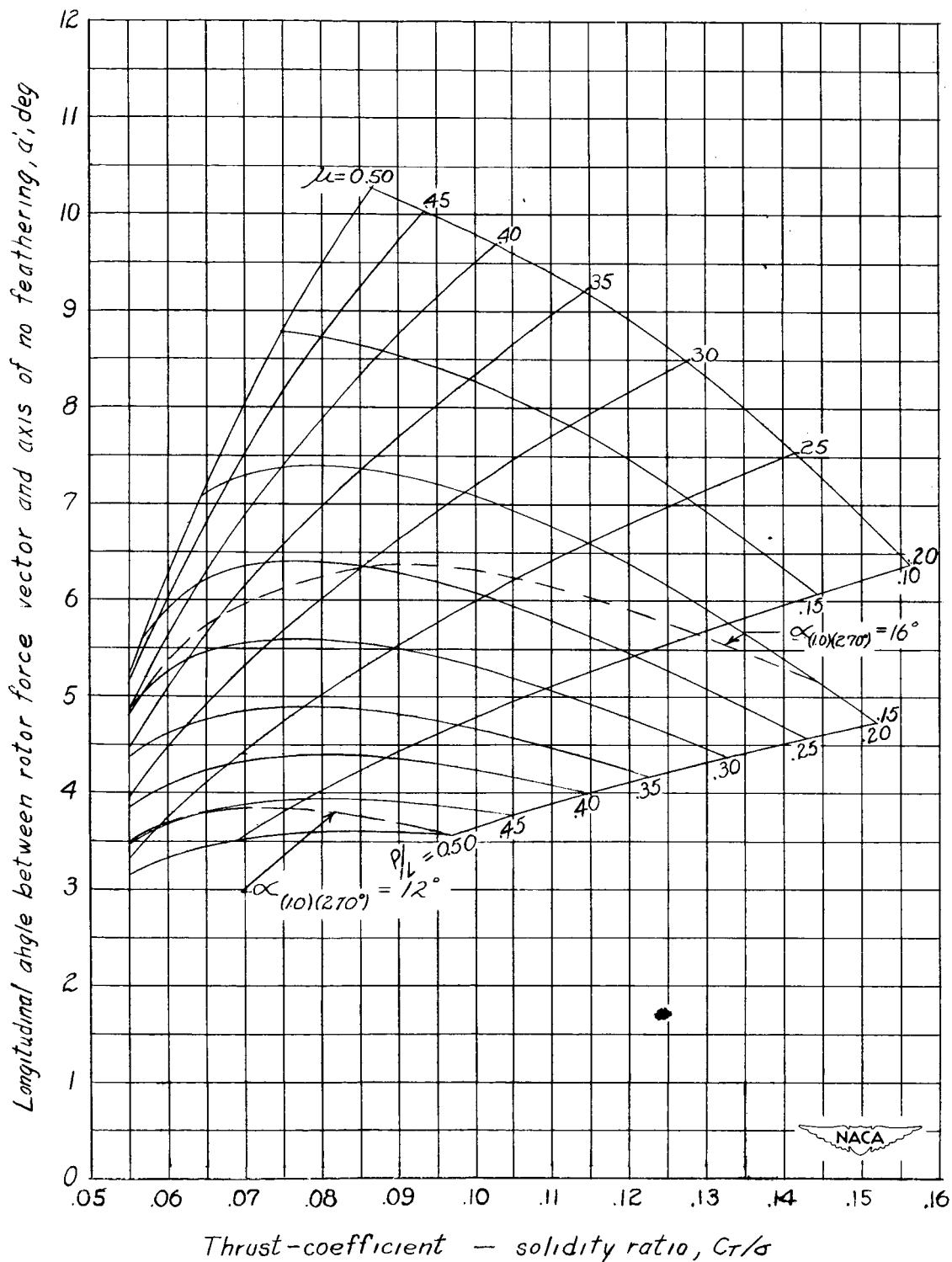
(g) $\theta = 12^\circ$.

Figure 3.- Continued.
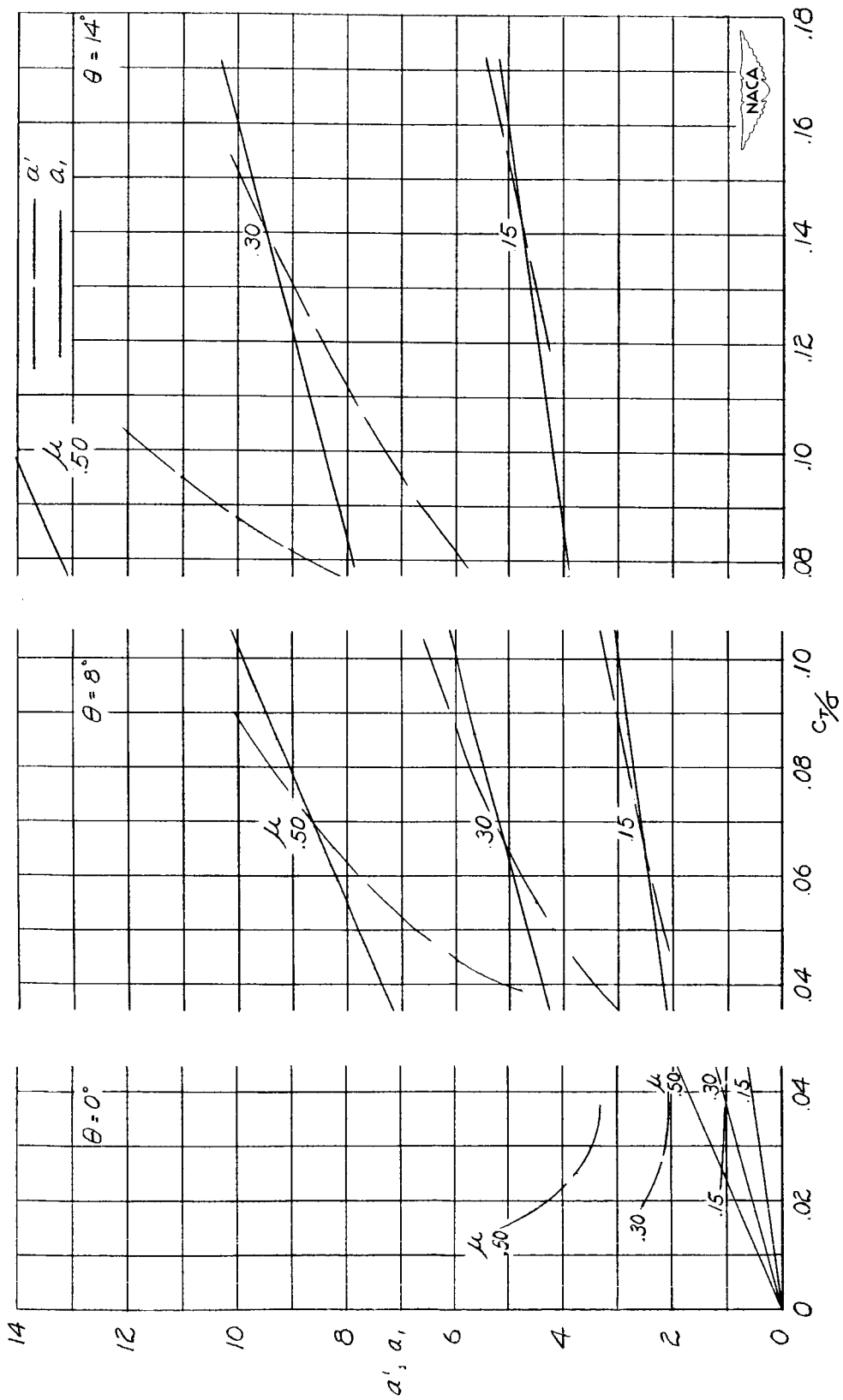
(h) $\theta = 14^{\circ}$.

Figure 3.- Concluded.

Figure 4.- Comparison between values of a_1 and a'.